12-2010

Protocol variation analysis of whole brain CT perfusion in acute ischemic stroke

Peter T. Heiberger
University of Nevada, Las Vegas

PROTOCOL VARIATION ANALYSIS OF WHOLE BRAIN CT PERFUSION IN ACUTE ISCHEMIC STROKE

by

Peter T. Heiberger

Bachelor of Science
University of Wisconsin, Eau Claire
2006

A thesis submitted in partial fulfillment of
the requirements for the

Master of Science in Health Physics
Department of Health Physics and Diagnostic Sciences
School of Allied Health Sciences
Division of Health Sciences

Graduate College
University of Nevada, Las Vegas
December 2010

UNLV
UNIVERSITY OF NEVADA LAS VEGAS

THE GRADUATE COLLEGE

We recommend the thesis prepared under our supervision by

Peter T. Heiberger

entitled

Protocol Variation Analysis of Whole Brain CT Perfusion in Acute Ischemic Stroke

be accepted in partial fulfillment of the requirements for the degree of

Master of Science in Health Physics
Department of Health Physics and Diagnostic Sciences

Steen Madsen, Committee Chair

Phillip Patton, Committee Member

Ralf Sudowe, Committee Member

Merrill Landers, Graduate Faculty Representative

Ronald Smith, Ph. D., Vice President for Research and Graduate Studies
and Dean of the Graduate College

December 2010

ABSTRACT

Protocol Variation Analysis of Whole Brain CT Perfusion in Acute Ischemic Stroke

by

Peter T. Heiberger

Dr. Phillip Patton, Advisory Committee Chair
Professor of Health Physics & Diagnostic Sciences
University of Nevada, Las Vegas

Computed tomography perfusion (CTP) analysis is a rapidly advancing imaging modality that is improving diagnosis of brain abnormalities in patients suffering from hemorrhagic or ischemic stroke, traumatic brain injury, vascular occlusion and numerous other conditions. Through the advancements of computed tomography (CT) imaging, including the introduction of the 320-detector row CT with a 16 centimeter range in the z-axis enabling whole brain CTP, perfusion analysis now has a significantly increased clinical utility that is useful for both diagnosis and treatment of central nervous system (CNS) conditions. This study focuses on the procedural and analytical approach to the diagnostic evaluation of patients suffering from acute ischemic stroke (AIS). Through the automatic, manual ipsilateral, and manual contralateral selection of the arterial input function (AIF) and venous input function (VIF), along with the interchangeable combinations using singular value decomposition (SVD) and singular value decomposition plus (SVD+) deconvolution algorithms, CTP parametric maps are compared and analyzed for similarities and differences between each selection method. In particular, the region of interest (ROI) placements on the axial views of the perfusion maps are compared with the values derived by the SVD+ and SVD deconvolution algorithms for each AIF/VIF selection. These differences and product CTP map manipulations allow for outcome

assessments that prove which approach provides the best clinical accuracy and reproducibility for evaluating or diagnosing acute ischemic stroke with computed tomography perfusion.

In this study of protocol variation analysis, SVD+ produced more consistent CTP values with less variation than the SVD deconvolution algorithm. With the use of the SVD+ deconvolution algorithm, the most consistent results were produced with the AIF manually placed in the contralateral M1 segment of the middle cerebral artery (MCA) and the venous input function (VIF) placed in the posterior portion of the superior sagittal sinus (SSS).

TABLE OF CONTENTS

ACKNOWLEDGEMENTS

I would like to thank everyone who was involved in the success of this research study and the compilation of this thesis. I would like to particularly thank the following people:

Dr. Eric H. Hanson MD, MPH

Dr. Phillip W. Patton Ph.D.

Cayce J. Roach BS

Kamran U. Haq MS

Additional thanks to the following:

Dr. Steen Madsen Ph.D.

Dr. Merrill Landers Ph.D.

Dr. Ralf Sudowe Ph.D.

I would also like to thank my parents and family for their continuous support through this educational experience.

CHAPTER 1

INTRODUCTION

1.1 Computed Tomography (CT)

Computed Tomography is a radiographic or medical imaging method used for the visualization of patient anatomy in two-dimensional and three-dimensional view. Planar cross-sectional x-rays are used for the creation of anatomical structures through the use of computer algorithms incorporating filtered back projection reconstruction. The x-ray source and corresponding detector make a complete 360-degree rotation around the patient to obtain a complete set of x-ray data for image reconstruction.[1] In order to increase the visibility of the organs and structures imaged during a CT scan, a contrast agent can be injected intravenously. This contrast will be taken up into the organs of interest and allow for a more defined and enhanced image of that anatomy. Some common contrast agents are barium, iodine, and water. These agents are effective as they have different x-ray absorption characteristics than soft tissue resulting in better contrast resolution density. The differences in attenuation of bodily organs due to their densities define the differences in Hounsfield Units. The Hounsfield Unit is calculated by using Eq. 1[1].

$$HU = 1000\left(\frac{\mu\,(x,y) - \mu\,water}{\mu\,water}\right) \qquad \textbf{Eq. 1}$$

where $\mu\,(x,y)$ is the linear attenuation coefficient of the (x,y) pixel and μ_{water} is the attenuation coefficient of water. The CT numbers range from about -1000 to +3000, where -1000 corresponds to air, soft tissues range from -300 to -100, water is 0, and dense bone and areas filled with contrast agent range up to +3000.

Multiple detector array CT scanners acquire multiple slices per rotation. The slice thickness is dependent on the number of active individual detectors or those detectors "binned" together. The use of a multiple detector array can decrease the slice width, which in turn can decrease the contrast resolution, but increases the spatial resolution for the depiction of finer detail. In the case of identification of AIS within the vasculature and tissue of the brain, spatial resolution is more important than contrast resolution. The reduction in contrast resolution can be compensated for by post-processing the acquired images through windowing and leveling.

Computed Tomography Perfusion (CTP) is the process of taking a CT of the vasculature of the brain, with the injection of a contrast agent. As the contrast agent travels through the vasculature, the CT imaging is initiated in order to acquire the scan simultaneously with the movement of the contrast agent. This allows for the visualization of the contrast through the vasculature to identify any form of blockage or thrombosis. In the case of AIS patients, the CT scan is acquired during the simultaneous entrance of the contrast into the brain. This method allows for the diagnosis and prognosis of stroke to a particular area of the brain.

CTP is possible due to the advent of multi-slice CT, along with the high resolution and high speed of the current scanners. Typical CT-angiography and perfusion have been done using a 64-slice (detector row) CT scanner allowing for a larger volume of acquisition. However, the limitation of field size with the 64-slice CT makes whole brain perfusion analysis difficult. With the introduction of Toshiba's Aquilion ONE 320-detector row CT, whole brain perfusion analysis is now possible.[2,8,9]

1.2 Acute Ischemic Stroke

This protocol analysis focused entirely on patients suffering from acute ischemic stroke. A stroke is a decrease or cease of blood to any particular area of the brain. This interruption of blood to the brain causes deprivation of oxygen to the brain tissue causing eminent necrosis of brain tissue.[3] Immediate medical care is to be sought at the onset of a stroke in order to spare and save as much brain tissue and brain function as possible.[4,5] The approach utilized to try and save tissue after the onset of stroke is to reopen the vasculature where the clotting has occurred. Some FDA approved drugs, such as tPA, are capable of revasculaturization.[6]

Ischemic describes a decrease in blood flow due to narrowing or blockage of an artery.[3,4] Ischemic includes both thrombotic and embolic stroke. Thrombotic occurs when one of the immediate arteries supplying blood to the brain is clotted causing a decrease or total blockage of blood flow. This is typically due to plaque build-up called atherosclerosis. Embolic stroke is due to the clotting of an artery elsewhere in the body and the clot dislodging itself only to clot in an artery feeding the brain. Therefore, acute ischemic stroke is defined as a sudden decrease or cease of blood flow to the brain due to a clot of the immediate blood supplying arteries to the brain.

The artery that clots the most frequently is the middle cerebral artery (MCA). This artery is one of two branches of the internal carotid artery and divides into three branches. It originates off of the internal carotid artery near the brain midline and branches bilaterally distal. The branches of the middle cerebral artery supply the extremities of the brain and engross a large volume of the brain. The posterior cerebral artery (PCA) may clot as well, although less frequently than the MCA. The posterior cerebral artery arises from the basilar artery and supplies oxygenated blood to the posterior portion of the brain

or the occipital lobe. Other arteries which clot less frequently but still result in a stroke are the basilar artery, internal carotid artery (ICA), and distal branches of both the PCA and MCA.

1.3 Research Goal

The goal of this comprehensive study was to identify the premier protocol for CTP analysis using the Aquilion ONE CT scanner (Toshiba Medical Systems, Nasu, Japan) along with the corresponding analysis software, Vitrea *fX* version 2.1 (Vital Images, Minnetonka, MN, USA). Identification of the most accurate and tested protocol can lead to a standard in the field of radiology in regards to analysis of AIS. CTP imaging is capable of providing physiological information leading to a rapid diagnosis and treatment of AIS. This immediate analysis via CTP of the patient anatomy allows for the identification of the infarcted core and the ischemic penumbra.[2] Thrombolytic drugs are available to reduce and ultimately remove the clot, but according to current FDA standards, must be administered within a three hour window following the onset of the acute ischemic stroke.[3,7] These imaging tools allow for individual diagnosis and prognosis and can tailor the treatment plan accordingly. Due to the individual patient's condition, the window for administering thrombolytic agents may be extended for increased tissue salvage.[8]

1.4 Brain CTP Analysis

AIS analysis for affected patients involves both the CT scanner and the Vitrea software consisting of dedicated convolution/ deconvolution algorithms for image recreation and manipulation. Understanding of the necessary inputs and variables of the software are also vital for understanding of the AIS analysis. In CTP imaging, the

contrast agent is injected intravenously and is scanned repeatedly (19 times for these patients) as the contrast travels through the brain tissue and vasculature. The Hounsfield Units are defined for each particular voxel, creating tissue-specific time density graphs.[10,11]

The current standard protocol for the Vitrea *fX* version 2.1 consists of a singular value decomposition deconvolution (SVD) algorithm. This algorithm consists of a delay-sensitive component for CT-Perfusion (CTP). Another algorithm that is being supplemented in place of the SVD algorithm is termed singular value decomposition plus deconvolution (SVD+). The SVD+ deconvolution algorithm consists of a delay-insensitive component for CTP. Vascular pixel elimination (VPE) is an option in the Vitrea *fX* program that is a mathematical tool used for pixel-smoothing. This allows for an averaging of neighboring pixels of varying values for a smoother value identification.

Singular value decomposition (SVD) is a non-iterative deconvolution method based on the central volume principle. This method solves convolution equations to determine a contrast residue function for each volume of interest.[10,12] The contrast residue function of the tissue is derived by deconvolution. Mean transit time (MTT) is determined from the width of the contrast residue curve. Imaging modalities such as magnetic resonance imaging (MRI), positron emission tomography (PET) and CT have adapted various forms of SVD-based deconvolution algorithms to calculate brain perfusion parameters. The SVD deconvolution algorithm, is capable and is utilized for deconvolving the tissue responses from the first pass of contrast to provide underlying vascular structure.[14] However, due to the high sensitivity to dispersion and delay in the arterial input curve, SVD may not accurately depict the true physiological changes that

are present in the individual patient.[13,21] This sensitivity to dispersion and delay will deconvolve perfusion maps that may not represent the true anatomical physiology, leading to a misdiagnosis of AIS. As the time to peak (TTP) and MTT are highly sensitive to hemodynamic changes in cerebral circulation, increased values of these parameters with normal CBF and CBV will not accurately identify infarction.[14,19] For example, an increase in TTP or MTT will be depicted with greater perfusion values on the perfusion maps, indicating to the reader that this is an area of possible infarction. This increase in perfusion values may just be a result of the high sensitivity to delay and dispersion, representing an inaccurate reading.[22,23]

To overcome the high sensitivity to delay and dispersion of the SVD deconvolution algorithm and the corresponding potential biological inaccuracies, the SVD+ deconvolution algorithm has been implemented.[15,18] This tracer delay insensitive method integrates an adjustment in which the arterial input function (AIF) is shifted and a preconditioning technique has been applied to make calculated perfusion parameters independent of the time of arrival of the bolus.[16,17] The bolus arrival time is set to zero at the first sign of arrival in the brain to avoid potential delay effects. The SVD+ algorithm provides the delay or the time in seconds when the calculated tissue residue function reaches the maximum. This CTP parameter of delay represents the difference in time of contrast arrival in the brain tissue and the arterial input function. This allows the SVD+ algorithm to avoid miscalculations due to dispersion and delay.

1.5 Variation of AIF and VIF Selections

The deconvolution methods of both SVD and SVD+ are directly responsive to the location selection of the arterial input function (AIF) and venous input function (VIF).

These locations allow for the creation of the corresponding arterial and venous bell curves in relation to the intensity of blood/ contrast versus time in seconds. Due to this relationship, CTP maps can vary drastically depending on the location of both the AIF and VIF. The location is indicative of the left or right hemisphere, the 'x' and 'y' coordinates within the 'z' axis and in which artery and vein the functions are placed. Unfortunately, due to the brevity of the technology used and the research within this field, there is no accepted standard for the selection of the AIF and VIF locations. Additionally, there is not an accepted standard for the selection site for particular neurological abnormalities and disease.

One must measure the accuracy and reproducibility of different selection sites to identify a premier approach for each individual AIS case analysis. As each reader approaches a case somewhat differently and has varying years of reading experience, variations will occur and need to be minimized as much as possible in order to create a standard. Several studies have shown that in comparison to the automatic AIF/VIF selection, the manual selection sites have a substantially lower variation percentage of perfusion values between multiple case analyses.[24] It is necessary to realize how much of an impact the deconvolution protocol and AIF/VIF factors have on individual cases in the clinical interpretation of the results.

1.6 Parameters Affecting Procedural Analysis

It is important to understand the CTP parameters that are used in each case analysis within the Vitrea fX software version 2.1. *Cerebral blood volume (CBV)* is the area under the computed residue function, adjusted by the brain concentration of contrast and the hematocrit constant. This is the volume of blood per 100 grams of brain tissue

(mL/ 100g). *Cerebral blood flow (CBF)* is the volume of blood flow per minute per 100 grams of brain tissue (mL/ min/ 100 g) and is calculated by CBV/ MTT. *Time to peak (TTP)* is the time in seconds between the start of the scan acquisition and the attenuation peak on the time-intensity graph. *Mean transit time (MTT)* is the average time in seconds for a bolus of blood to cross the capillary network in a given amount of tissue. *Delay* is the difference in time of contrast arrival in the brain tissue and the AIF. It is independent of the scan start time and contrast injection time or rate. It is measured as the time in seconds for the computed residue function to reach a maximum and is available in SVD+ and SVD software, but is not reported in SVD literature.[26]

In order to measure the response of the selection variability of the AIF and VIF, a product map of the CBV and CBF parameters is created. Lee et al[25] found that the CBF x CBV product map created a qualitative CTP map that enhanced the differences between the penumbra and infarct core better than the CBV or CBF threshold alone. The CBF x CBV product map was created by multiplying the value of a gray matter (GM) and white matter (WM) pixel on the CBV map by the value of the corresponding pixel on the CBF map.

CHAPTER 2

MATERIALS AND METHODS

This study is a retrospective anonymized study of CT scans that were obtained for clinical purposes. Twenty-four randomized patients evaluated at a high volume stroke center were reviewed. Seven patients demonstrated both clinical and radiographic evidence of non-hemorrhagic stroke. Table 1 lists the case findings of the two men and five women with signs and symptoms of AIS. Each received a whole-brain CT on the day of admission. Personal information that would identify the patient was not used in analysis or interpretation of the data.

Table 1. Age, gender, AIS locations and arterial occlusion sites for the seven AIS cases.

Case	Age and Gender	AIS Location	Arterial Occlusion Site
1	58-year-old male	Lateral aspects of left posterior frontal lobe and parietal lobe	Left middle cerebral artery
2	88-year-old female	Left superior frontal lobe	Left anterior cerebral artery
3	80-year-old female	Right frontal lobe infarcts and chronic subdural hematomas	Right internal carotid artery
4	92-year-old female	Left anterior frontal lobe	Left distal middle cerebral artery
5	87-year-old male	Right frontal lobe	Right middle cerebral artery
6	60-year-old female	Left frontal lobe	Left middle cerebral artery
7	67-year-old female	Right inferior frontal lobe	Right middle cerebral artery

2.1 Image Acquisition

All image acquisitions utilized the Toshiba 320-detector row CT scanner and a non-contrast CT (NCCT) was initially completed to rule out hemorrhagic stroke or blood brain barrier breach, followed by the contrast scan. The contrast agent (primarily iodine) was intravenously injected into an antecubital vein at a rate of 6 mL/s. As the contrast travelled through the vasculature, a one-second scan was taken in every one-second interval for the first thirteen acquisitions of the arterial vasculature. Then a one-second scan was taken every five seconds during the progression through the venous vasculature for a total of five additional scans. The scans were conducted with an initial 310 mA mask followed by a 150 mA series for 4 acquisitions, 300 mA series for 5 acquisitions, and 150 mA series for 4 acquisitions during the arterial vasculature, and 150 mA series for 5 acquisitions during the venous vasculature. The voltage was 80 kVp with a 320 detector array resulting in a 160 mm field coverage. Each of the 320-detector rows was 0.5 mm in width. The Vitrea fX version 2.1 software utilizing SVD+ was compared with a standard SVD algorithm configuration that is not commercially available in the same software. The radiation doses were estimated using the dose length product (DLP) obtained from the CT console. DLP values were then converted to effective dose by applying the conversion factor for CT of the head (DLP x 0.0023) according to the European Guidelines for Multislice CT.[27] Table 2 lists the scanning configurations and protocol that was consistently used for each patient.

Table 2. 320-detector row CT hardware, software, protocol and scan configurations parameters.

CT configuration	320 x 0.5 mm detector row
Contrast amount (mL)	50
Contrast infusion rate (mL/sec)	6
Section thickness	0.5 mm with 0.5 mm interval
Kilovolts (kVp)	80 kVp
Milliamp (mA)	Initial 310 mA mask; arterial – 150 mA series for 4 acquisitions, 300 mA for 5 acquisitions, 150 mA for 4 acquisitions – all arterial occur every other second; venous – 150 mA for 5 acquisitions 5 seconds apart
Size of detector array (FOV)	160 mm
Software and version	Vitrea *fX* software version 2.1
Brain analysis software mode (2D or 4D)	Brain Analysis CT, 4D Perfusion
Deconvolution algorithm utilized	SVD+ or SVD
Singular value decomposition (SVD) deconvolution cutoff threshold	5%
Vascular pixel elimination (VPE)	VPE on (default setting)
DLP to milliSieverts (mSv)	5.9 mSv
AIF and VIF selection location	Varied automatic selection by Vitrea *fX* software, ipsilateral (ipsi) manual or contralateral (contra) manual selection

2.2 CTP Data Collection and Initial Analysis

Analysis of the quantitative and qualitative differences between the SVD+ and SVD deconvolution algorithms with the selection variations of the AIF and VIF allowed for the identification of the most accurate and reproducible reading protocol using the Vitrea fX version 2.1 software. In order to do this, the voxel data sets at each slice level

were analyzed using MATLAB (The Mathworks, Inc., Natick, Massachusetts, USA) .The analysis of these slice voxel data sets allowed for the measurement of the differences visualized using both 2-D and 3-D graphical representations.

A 2D and 3D colorimetric perfusion map was created using MATLAB to qualitatively compare the differences between the SVD+ and SVD deconvolution algorithms. These qualitative comparisons show the changes in perfusion values as well as the clarity and smoothness of the images.

2.3 Comparison of SVD+ and SVD by Linear Pixel Graphs

This comparison involved using the MATLAB *IMPROFILE* function to manually draw a line through the infracted core. This 2D line manually extended from tissue beyond the penumbra, across the penumbra, through the infarct core, back into the penumbra, and then into the tissue beyond the penumbra. The "*IMPROFILE*" function then calculated the linear pixel intensity values selected for equally spaced points in relation to the line. The MATLAB program generated a 2D graph of pixel versus CBF x CBV[28] values based on the manually created line across the infarct.

2.4 AIF and VIF Selection Variation

When each case is initialized on the Vitrea fX software to be analyzed, the software automatically selects the AIF and VIF locations to best create the perfusion maps. To measure the differences in AIF/VIF selections, the AIF and VIF was manually placed both ipsilaterally and contralaterally to the infracted hemisphere. The AIF was placed in the MCA as well as the PCA for comparison and the VIF will be placed in the superior sagital sinus (SSS) and the confluence of dural venous sinuses (CDVS) for

comparison. These variations will be analyzed in both the SVD+ and the SVD deconvolution algorithms.

To investigate the variation of the SVD+ and SVD with AIF, the manual AIF selection of the contralateral MCA was compared to the manual contralateral PCA while the VIF will be held constant in the SSS using SVD+ and then SVD. The 2D and 3D colorimetric maps were created to qualitatively assess the clinical interpretation.

Using the CBF x CBV mapping approach, the automatic VIF selection in the CDVS was compared with the manually selected SSS location. The AIF was held constant in the M1 segment of the MCA. The comparison was evaluated using the 2D and 3D colorimetric graphs created by MATLAB for both the SVD+ and SVD deconvolution algorithms.

2.5 CBF Linear Pixel Subtraction Graphs

In order to verify results, subtraction mapping was used to compare the differences between variations of the AIF/ VIF selection locations. The manually selected AIF in the ipsilateral and contralateral MCA was subtracted from the automatically selected AIF/ VIF location. Also, the manually placed contralateral PCA was subtracted from the automatic selection. These manually selected AIF locations were held constant with the VIF placed in the SSS. This was performed with both the SVD+ and SVD deconvolution algorithms.

In order to determine the influence of the SSS on the CBF, VIF placement was held constant and a 2D linear pixel subtraction graph of CBF variation was created by subtracting the automatic CDVS (automatic AIF in the contralateral PCA) from the manual CDVS VIF selection (AIF in the contralateral MCA).

In order to show that the variations are due to selection of different vessels and not secondary to small changes in selection location or software deviations, subtraction graphs were generated. The operator-placed input functions were placed in the exact same location as the automatic. The slight differences in placement location in comparison to the automatic placement showed a very small deviation in the results. Secondly, the same case with the same exact AIF/ VIF locations was brought up on two separate workstation consoles at different times and compared for similarities and variations between the two consoles. This helped to show reproducibility within the study.

All seven of the AIS cases were analyzed along these pre-mentioned guidelines and the 2D and 3D images and graphs were shown respectively per each case analysis.

2.6 Dose Reduction Analysis

Decrease in radiation exposure is a vital component in regards to any imaging modality and will be evaluated with the elimination of one or more volume acquisitions of the CTP. The current scanning protocol consists of 19 volume acquisitions from the beginning non-contrast volume acquisition through the last volume acquisition at approximately 53 seconds from the start of the scan. The time-intensity graph shows the bell curve of the arterial and venous curves to tail off with the continuation of time. Removing a volume acquisition from the end of the scan may show the same qualitative parameters as the scan with all 19 volume acquisitions.

In an attempt to reduce the exposure to the patient, the previously analyzed data were compared to data created from removing 1-5 acquisitions of the whole-brain CT imaging protocol. Removing the last volume acquisition may not affect the perfusion

physiology of the patient in a substantial way and thus allow for a reduction in the exposure to the patients in the future.

Seven patients were used to measure these differences. Qualitative analysis was done between the full volume acquisition scan versus the scan with acquisitions removed. The scans were analyzed to see if any vital anatomical or physiological information is missing for an accurate clinical interpretation.

The DLP values given by the CT console are calculated by the DLP equation given in Eq. 2[1].

$$\text{DLP} = \sum CTDIw \times Ti \times Ni \text{ (mGy*cm)} \qquad \textbf{Eq. 2}$$

where $CTDI_{wi}$ is the computed tomography dose index number, T_i is the thickness of the slice, and N_i is the number of slices. The CTDI is measured using a long (100 mm), thin pencil ionization chamber within the CT scanner. In order to calculate the CTDI, all of the energy deposition along the length of the ion chamber is assigned to the thickness of the CT slice. Therefore, the CTDI value of the DLP equation is given in units of mGy, which is the result of the exposure-to-dose conversion.

CHAPTER 3

RESULTS

3.1 Analysis of Colorimetric CTP Maps and CBF x CBV Threshold

The colorimetric CTP maps of Case 1 for CBV, TTP, CBF and MTT generated using SVD+ (Fig. 1) and using SVD (Fig. 2) delineated areas of infarction and hypoperfusion within the MCA distribution of the right hemisphere of the brain. The CBV map (Fig. 1b and 2b) shows the hypoperfused areas in the blue indicating a decrease in blood volume to that particular area. The CBF map (Fig. 1d and 2d) shows the same areas slightly hypoperfused as well with the blue pixel color indicating a decreased blood flow to that area. The same areas of hypoperfusion on the CBV and CBF maps show an area of hyperperfusion on the TTP maps (Fig. 1c and 2c) indicating an increased time to peak area. The MTT maps (Fig. 1e and 2e) show the area to be slightly hypoperfused indicating a decrease in mean transit time. All of the results of the hypoperfusion and hyperperfusion with the corresponding maps indicate a possibility of infarction or stroke area. The contrast CT (Fig. 1a and 2a) revealed a nonhemorrhagic anatomical distribution of the infarcted and ischemic tissue in the right side deep grey matter. There was also evidence of infarcted tissue in the cortical grey matter of the frontal, parietal, and temporal lobes, along with the white matter of the posterior parietal lobe.

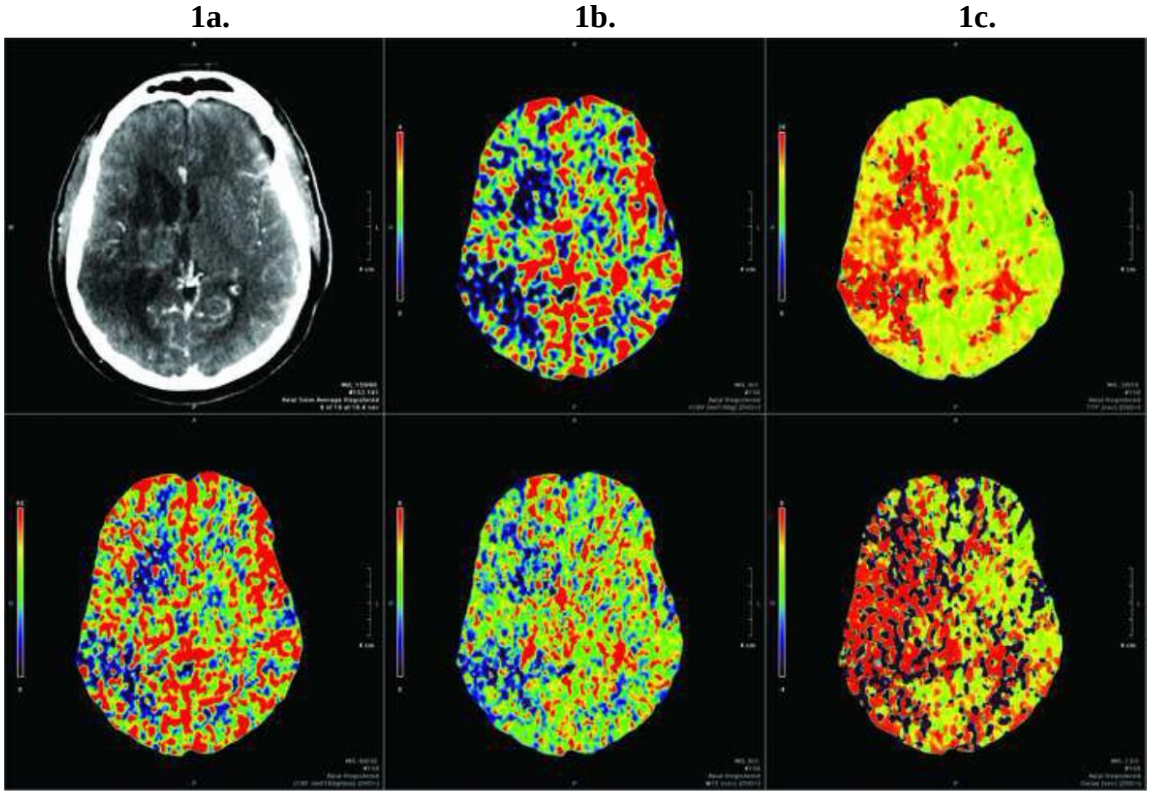

Figure 1. Contrast CT image and colorimetric CTP maps of the slice level of the fronto-parietal operculum utilized for analyses of Case 1. Contrast CT demonstrates extensive HU signal changes in the right MCA distribution indicating involvement of right side deep gray matter, genu and posterior limb of the internal capsule, cortical gray matter of the frontal, parietal and temporal lobes and the posterior parietal white matter. Colorimetric CTP maps for CBV, TTP, CBF, MTT, and delay generated using SVD+ with manual contralateral AIF selection at the M1 segment of MCA, and manual VIF selection at the posterior third of the posterior SSS.

2a. **2b.** **2c.**

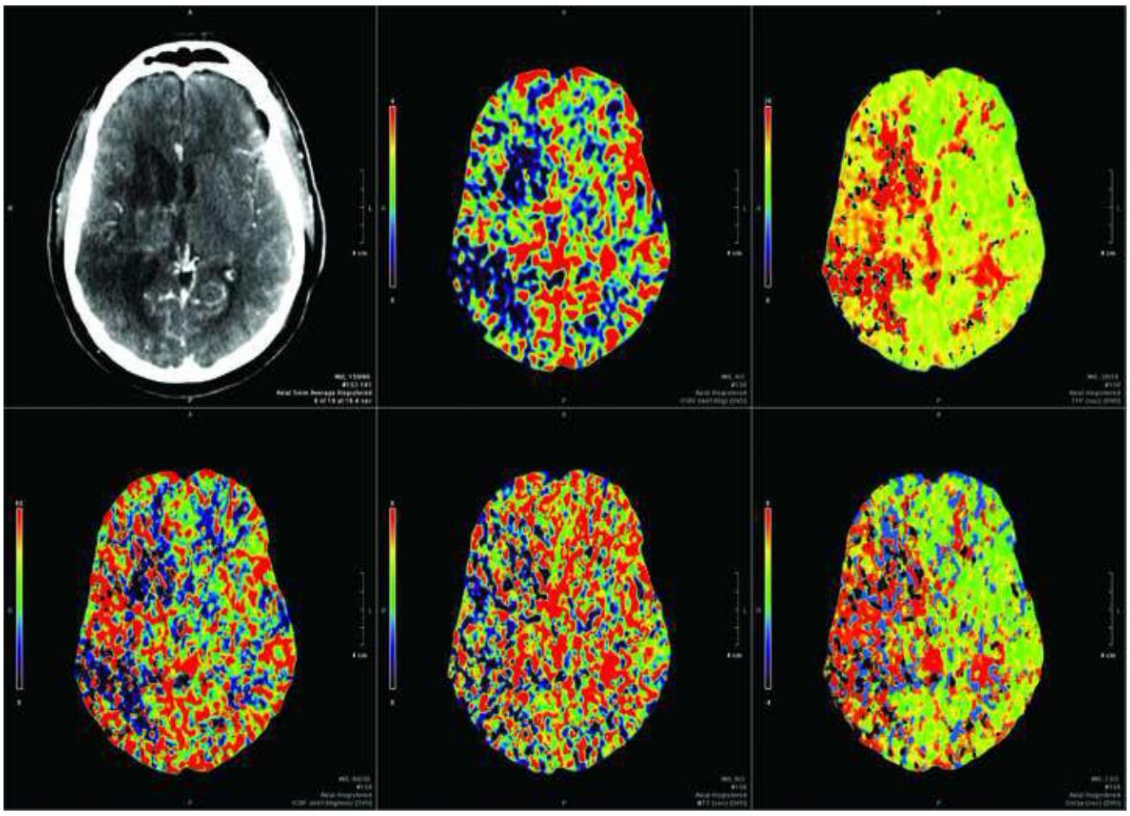

2d. **2e.** **2f.**

Figure 2. Contrast CT image and colorimetric CTP maps of the slice level of the fronto-parietal operculum utilized for analyses of Case 1. Contrast CT demonstrates extensive HU signal changes in the right MCA distribution indicating involvement of right side deep gray matter, genu and posterior limb of the internal capsule, cortical gray matter of the frontal, parietal and temporal lobes and the posterior parietal white matter. Colorimetric CTP maps for CBV, TTP, CBF, MTT, and delay generated using SVD with manual contralateral AIF selection at the M1 segment of MCA, and manual VIF selection at the posterior SSS.

The comparisons of the CTP colorimetric maps generated with SVD+ (Fig. 1) and with SVD (Fig. 2) were qualitatively similar for CBV and TTP, while CBF using SVD+ appears to have higher overall collateral flow than SVD, which is shown by the higher perfusion around the perimeter of the infarcted area on the CBF map. On the 2D "slice

voxel" map (Fig. 3), it is qualitatively apparent that SVD had increased collateral circulation and global perfusion increases outside the infarct compared to SVD+ on automatic contralateral (VIF in the CDVS) and manual ipsilateral AIF (VIF in the posterior SSS) selections of the PCA. In regards to the manual contralateral MCA (VIF in the posterior SSS) however, the CBF x CBV product values for collateral and global using SVD+ were higher than SVD.

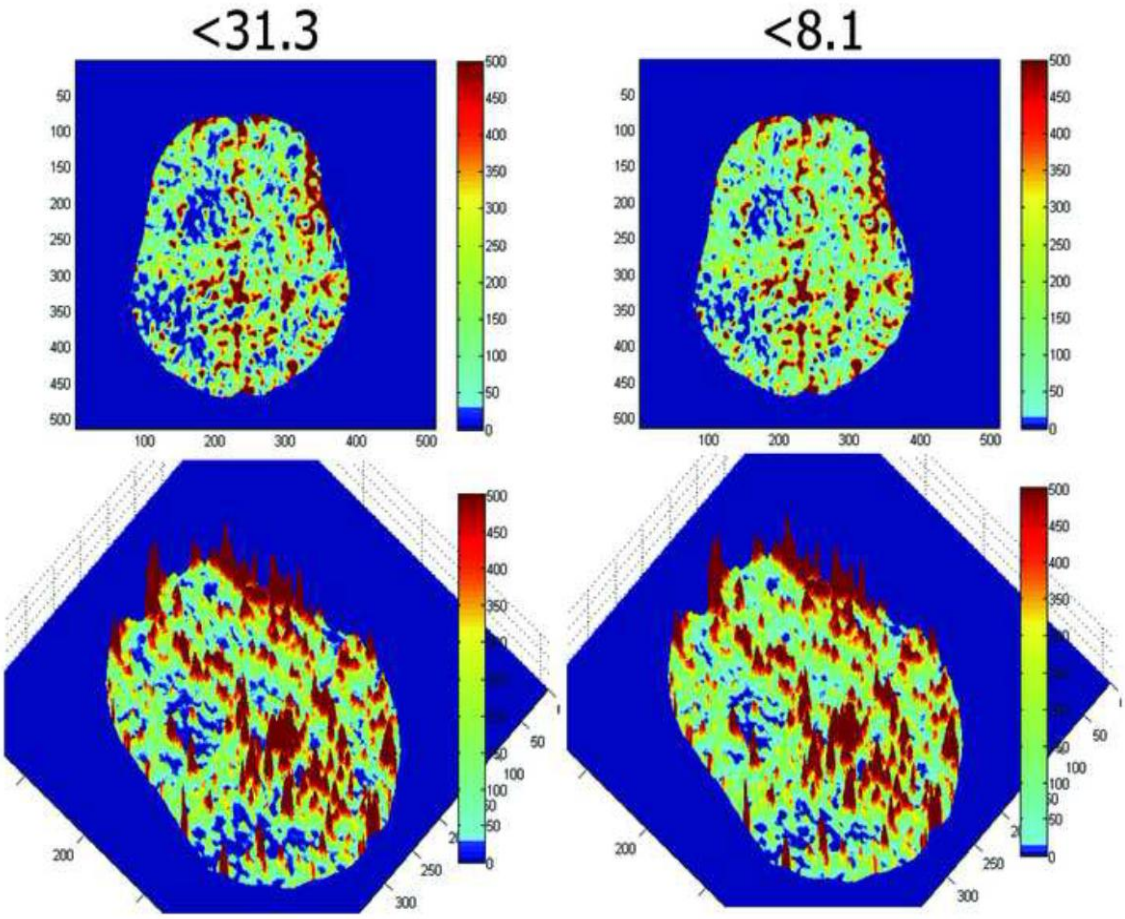

Figure 3. 2D and 3D "slice voxel" maps of CBF x CBV product values in Case 1. Blue regions denote CBF x CBV product values less than 31.3 (left) and less than 8.1 (right). AIF selection is in the contralateral MCA and VIF selection is in the posterior SSS. SVD+ is the deconvolution protocol.

According to a study by Lee et al.[25], the CBF x CBV value of 31.3 is the cutoff from the recovering penumbra to the infarcted penumbra in regards to the grey matter (GM). Therefore, any pixel value in the grey matter less than 31.3 has a higher probability to lead to infarct core tissue (non-recovering) and any pixel value in the grey matter greater than 31.3 has a higher probability of recovery. This same study indicated a cutoff threshold of 8.1 for white matter. Comparison of the Case 1 CTP colorimetric maps (Fig. 1) and the 2D "slice voxel" map (Fig. 3) with SVD+ using the 31.3 range threshold for grey matter, revealed an area of ischemia most resembling the CBV perfusion map (Fig. 1b). This ischemia pattern was also apparent but to a lesser degree in the CBF (Fig. 1d), MTT (Fig. 1e) and TTP (Fig. 1c) maps, respectively. Further analysis of the ischemic and infarcted areas for Cases 1-7 below utilized the higher threshold for CBF x CBV value less than 31.3 for GM due to the high proportion of cortical and deep GM involved in Case 1 (Fig. 3) that is again, more extensively described in the article by Lee et al.[25]

3.2 SVD+ versus SVD Impact on CTP Values

In general, SVD+ produced more consistent CTP values with less variation than SVD based on several different comparisons. The standard deviation of the automatic AIF/VIF selection for the SVD generated maps compared to the SVD+ generated maps was three times greater in regards to the average pixel over the entire area of the perfusion map. The p-value was less than 0.001, which indicates a significant difference between the two subsets of SVD+ and SVD. The 95% confidence interval was between 44.75 and 47.64 with the mean difference of 46.20, which shows a very small margin of variability. One qualitative comparison of 2D "slice voxel" CBF x CBV values with

varying the AIF and VIF selections resulted in the SVD+ colorimetric maps to have less color variation and more contiguous mapping results between case studies in comparison to the SVD colorimetric maps (Fig. 4). Another comparison consisted of quantitative 2D "linear pixel" graphs showing less variation in CBF x CBV product values to facilitate presumed infarct and penumbral identification.

Comparison between SVD and SVD+ in regards to the 3D "slice voxel" CBF x CBV product perfusion maps (Fig. 5) resulted in a greater variation of CTP values within the core and surrounding penumbral tissue in SVD and more consistency with less variation perfusion map in SVD+. Infarct core areas using SVD+ are shown in Figures 1 and 3. SVD+ generated a CBF x CBV product map with increased peaks (taller) that were similar to the results in the manual ipsilateral AIF selection of the PCA and the manual contralateral selection of the MCA. This is most likely due to the consistent selection of the VIF in the posterior SSS. SVD generated a CBF x CBV product map with sporadic peaks and very inconsistent perfusion values throughout the perfusion area with similar AIF selections but in opposing hemispheres (automatic contralateral PCA selection and manual ipsilateral PCA selection).

Comparison of the 2D "linear pixel" graphs created in result of the CBF x CBV product maps (Fig. 6) indicated differing results between SVD and SVD+. Both graphs tend to show the presumed infarct core and penumbral boundaries with corresponding peaks, but the SVD-generated graphs show several and inconsistent peaks, with SVD+ generated graphs showing greater consistency. The SVD+ protocol defined the bordering ischemia with increased CBF x CBV values as sharp or smooth single peaks for each of the automatic, ipsilateral manual and contralateral manual AIF/VIF selections. SVD had

multiple peaks on each side of the infarct and large variation in quantitative values (Fig. 7).

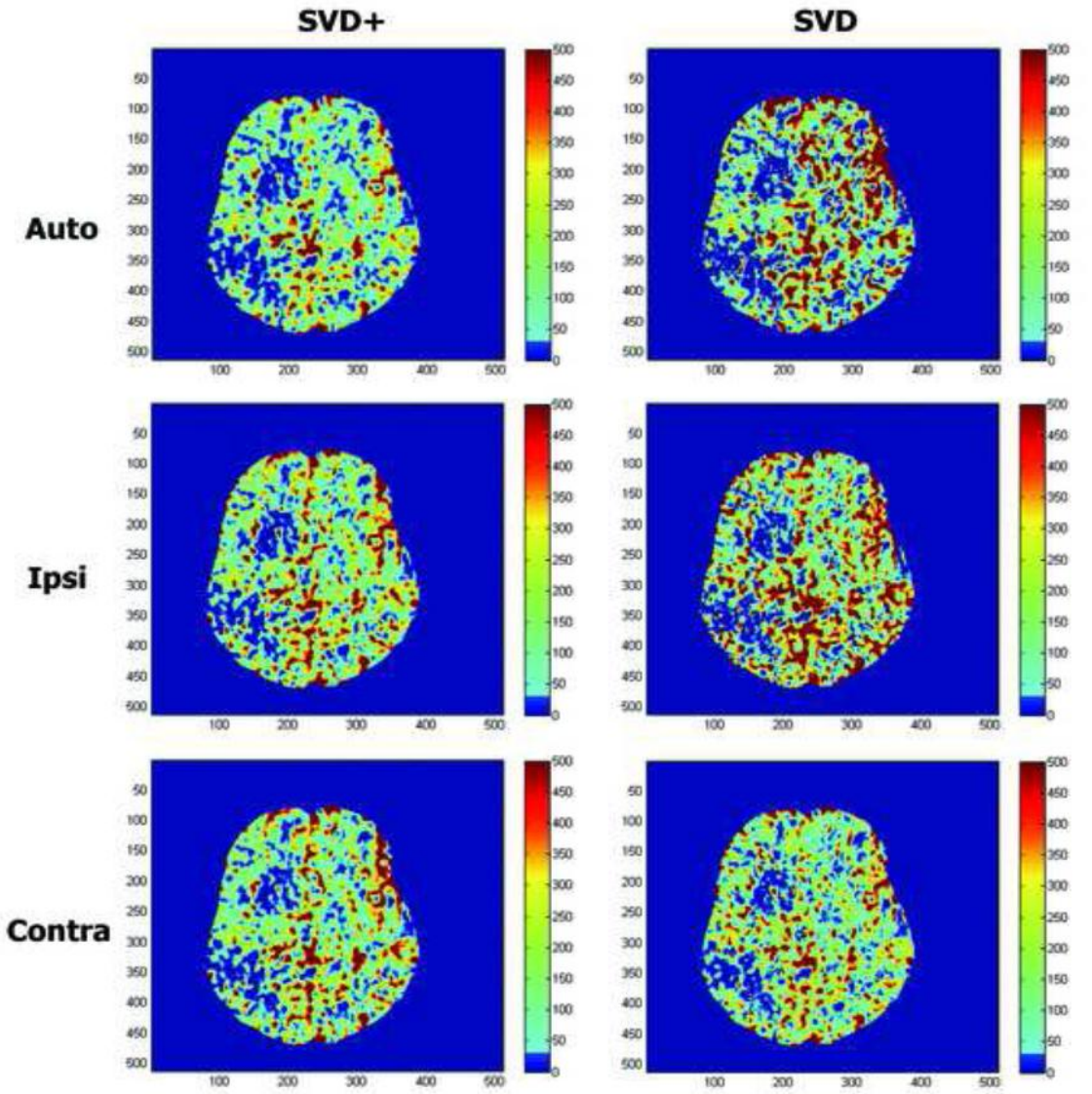

Selection	Automatic (Auto)	Ipsilateral (Ipsi)	Contralateral (Contra)
Arterial (AIF)	Contralateral PCA	PCA	MCA
Venous (VIF)	CDVS	SSS	SSS

Figure 4. 2D "slice voxel" comparison of CBF x CBV. Qualitative comparison of colorimetric map outputs for automatic, ipsilateral and contralateral AIF/VIF selections and SVD+ or SVD.

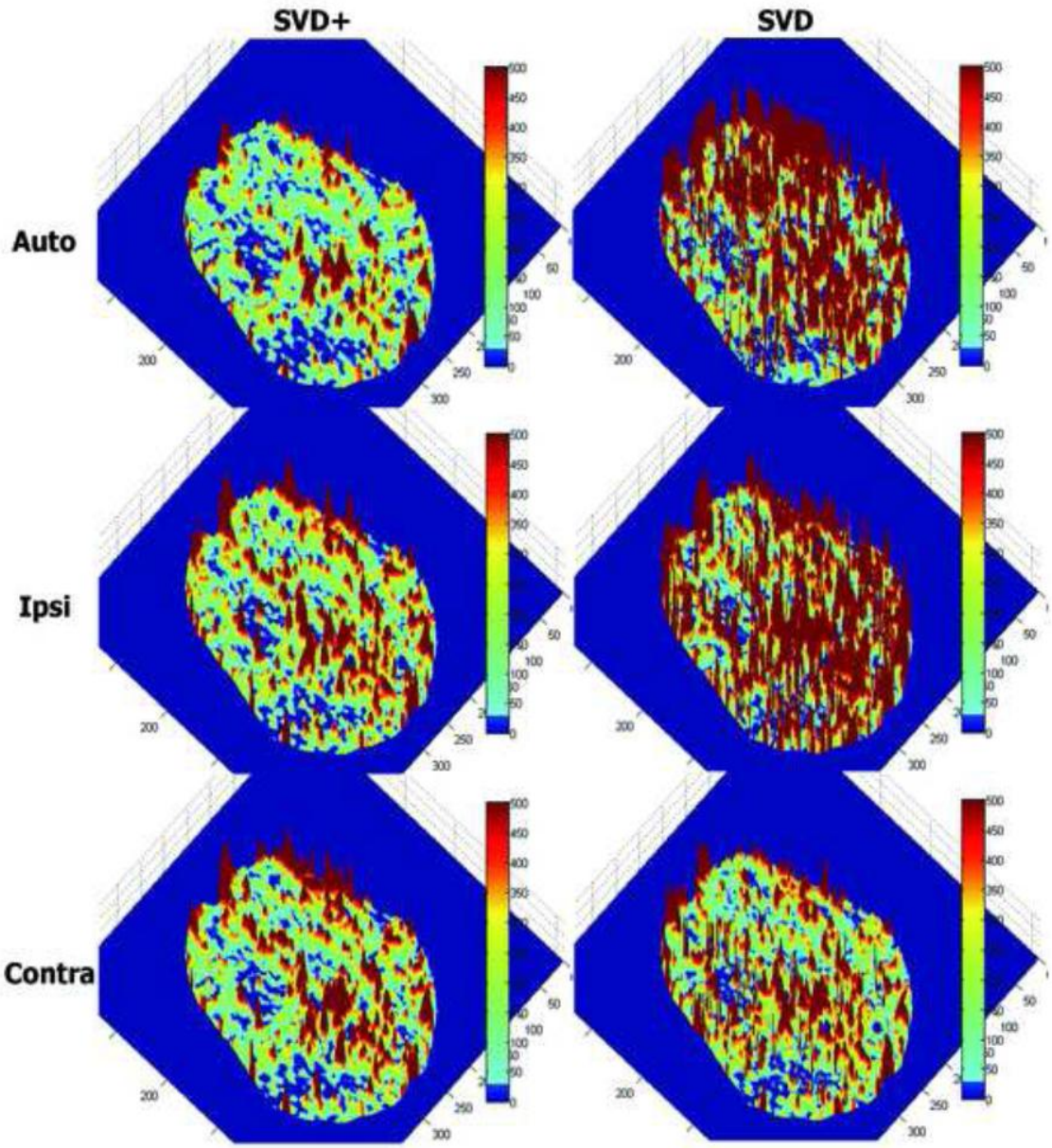

Selection	Automatic (Auto)	Ipsilateral (Ipsi)	Contralateral (Contra)
Arterial (AIF)	Contralateral PCA	PCA	MCA
Venous (VIF)	CDVS	SSS	SSS

Figure 5. 3D “slice voxel” CTP maps generated for the CBF x CBV product map to add a visual factor that can aid in the clinical interpretation process. 3D "slice voxel" colorimetric maps were created to compare variation in a 3D format of CBF x CBV value outputs based on AIF/VIF and SVD+/SVD variations.

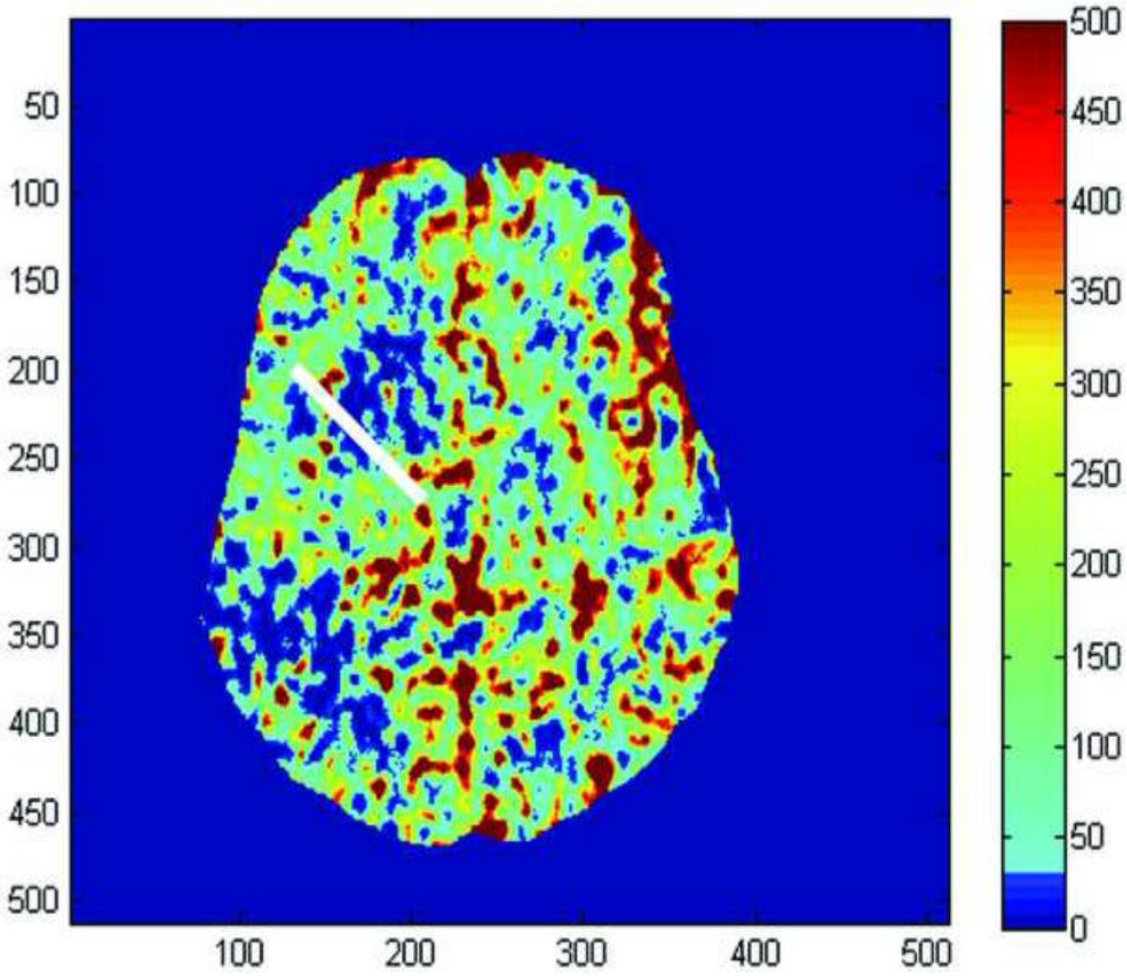

Figure 6. The "linear pixel" approach consists of a white line drawn by the reader across surrounding brain tissue, ischemic penumbra, homogenous area of the infarct core, ischemic penumbra and surrounding brain tissue to select a linear set of pixels. The linear set of pixel values are then transformed into graphs as depicted in Figure 7, 10, 13, and 14.

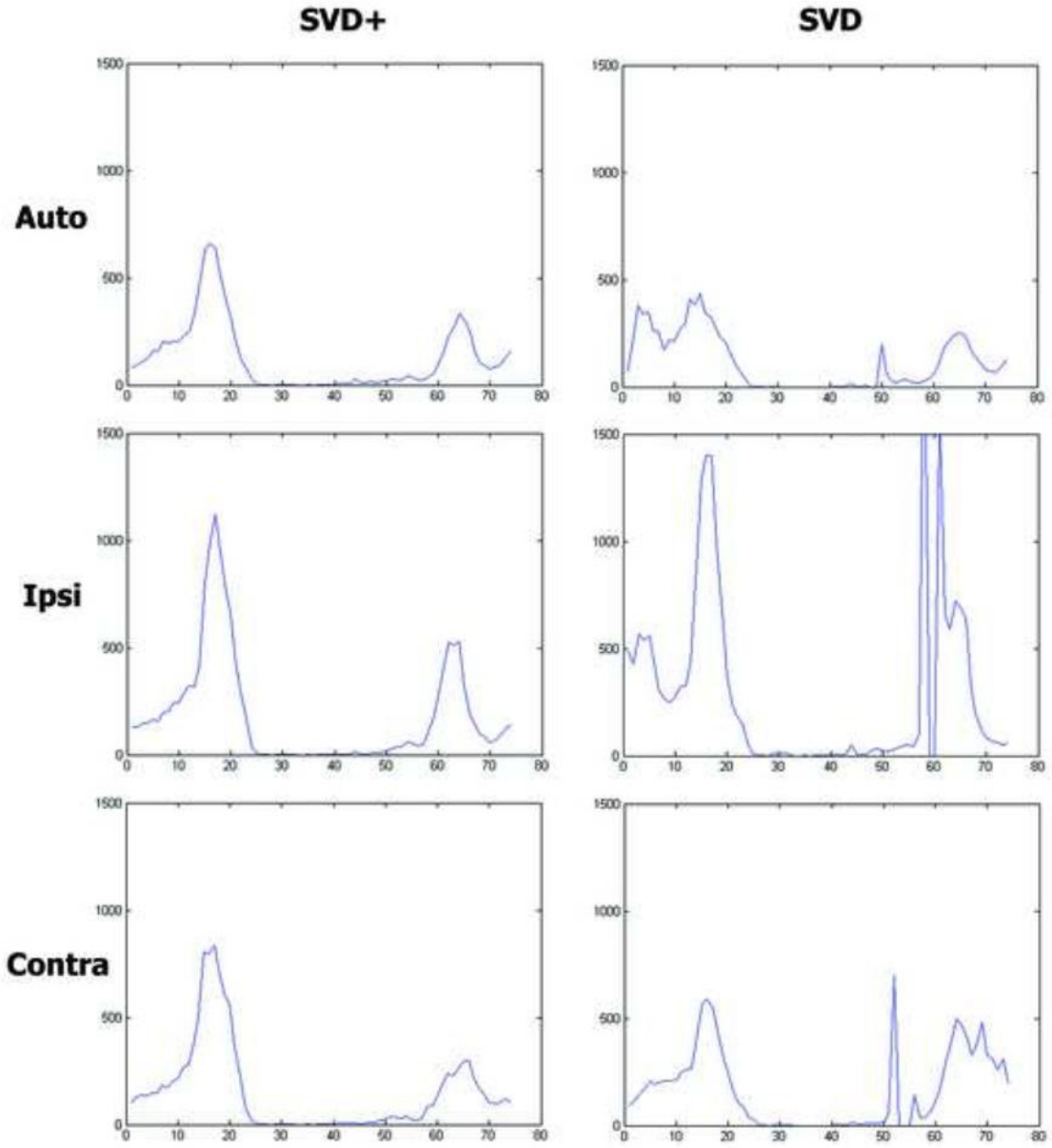

Selection	Automatic (Auto)	Ipsilateral (Ipsi)	Contralateral (Contra)
Arterial (AIF)	Contralateral PCA	PCA	MCA
Venous (VIF)	CDVS	SSS	SSS

Figure 7. 2D "linear pixel" graphs created to compare variation of CBF x CBV value outputs based on AIF/VIF and SVD+/SVD variations. The graphs depict CBF x CBV values versus pixel length across an infarct core as drawn in Figure 5. Each pixel value represents 0.5 mm. The y-axis is the product of CBF x CBV pixel values at the same location. The x-axis is 80 linear pixels collected in the linear selection ROI moving from lateral superior to the medial inferior aspects for the frontal lobe infarct.

3.3 Varying Location of AIF Selection (VIF Held Constant)

Varying the AIF location between the MCA and PCA produced differences in the CBF x CBV product values for both SVD+ and SVD. Results indicated less variation in CTP values between changes of AIF location when the SVD+ protocol was used in comparison to the SVD protocol (Fig. 8). The comparison of the AIF selections in the manual contralateral PCA and MCA generated CBF x CBV product maps with similar results. In the 2D "slice voxel" maps, the manual contralateral selection of the AIF in the PCA showed a much more variable and less defined infarct core area for qualitative analysis for both the SVD+ and SVD protocols (Fig. 8). The 3D "slice voxel" maps showed the MCA selection to produce more defined peaks compared to the PCA selection because the higher overall perfusion values in the MCA are more easily visualized in 3D (Fig. 9). Overall, the CBF and CBV values are increased by selecting the MCA over the PCA. Using SVD, there was more variation in the CBF x CBV product values and more poorly defined peaks than SVD+ (Fig. 10).

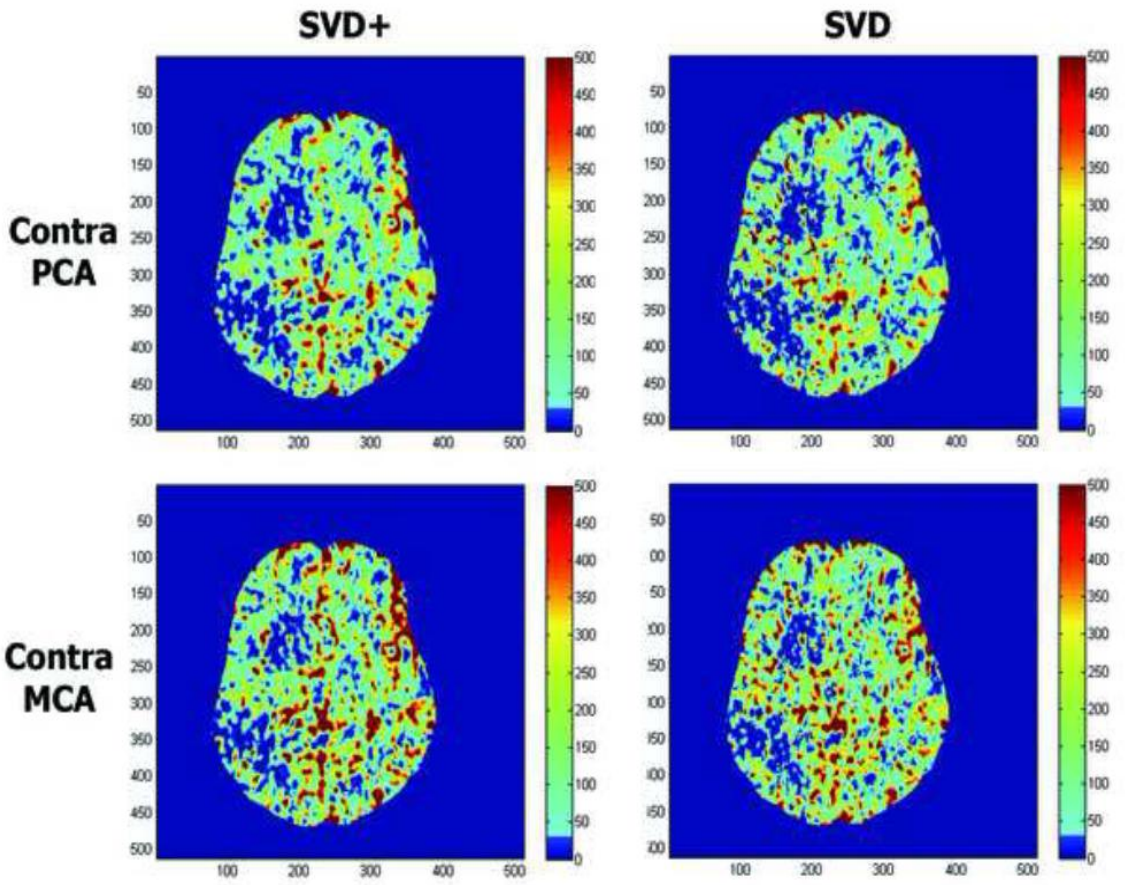

Selection	Contralateral Variation 1 (Contra PCA)	Contralateral Variation 2 (Contra MCA)
Arterial (AIF)	PCA	MCA
Venous (VIF)	SSS	SSS

Figure 8. Varying the arterial location of the AIF selection. 2D "slice voxel" representation of changing the contralateral arterial position between posterior cerebral artery (PCA) and the middle cerebral artery (MCA) for CBF x CBV value outputs based on AIF/VIF and SVD+/SVD variations.

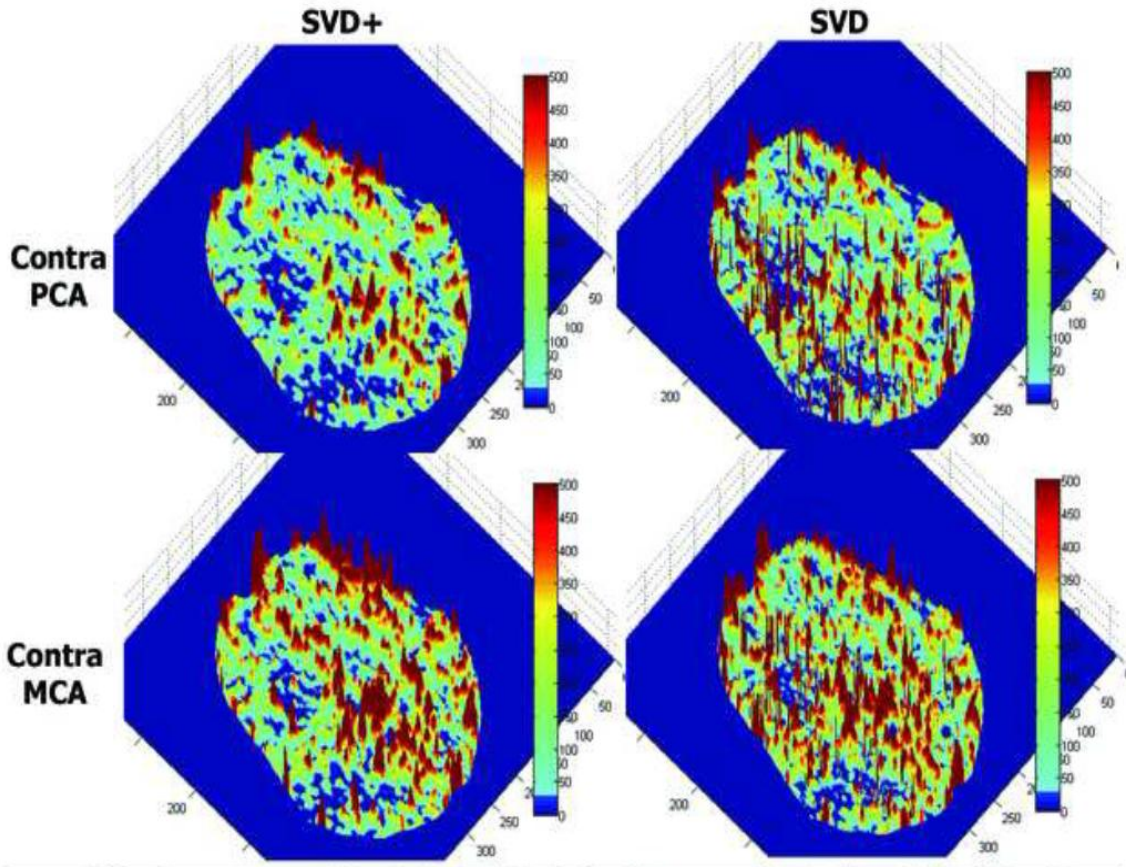

Selection	Contralateral Variation 1 (Contra PCA)	Contralateral Variation 2 (Contra MCA)
Arterial (AIF)	PCA	MCA
Venous (VIF)	SSS	SSS

Figure 9. 3D "slice voxel" colorimetric maps created to compare variation in a 3D format of CBF x CBV product values based on varying the AIF location either in the PCA or MCA (VIF held constant in the posterior SSS) and SVD+/SVD variations.

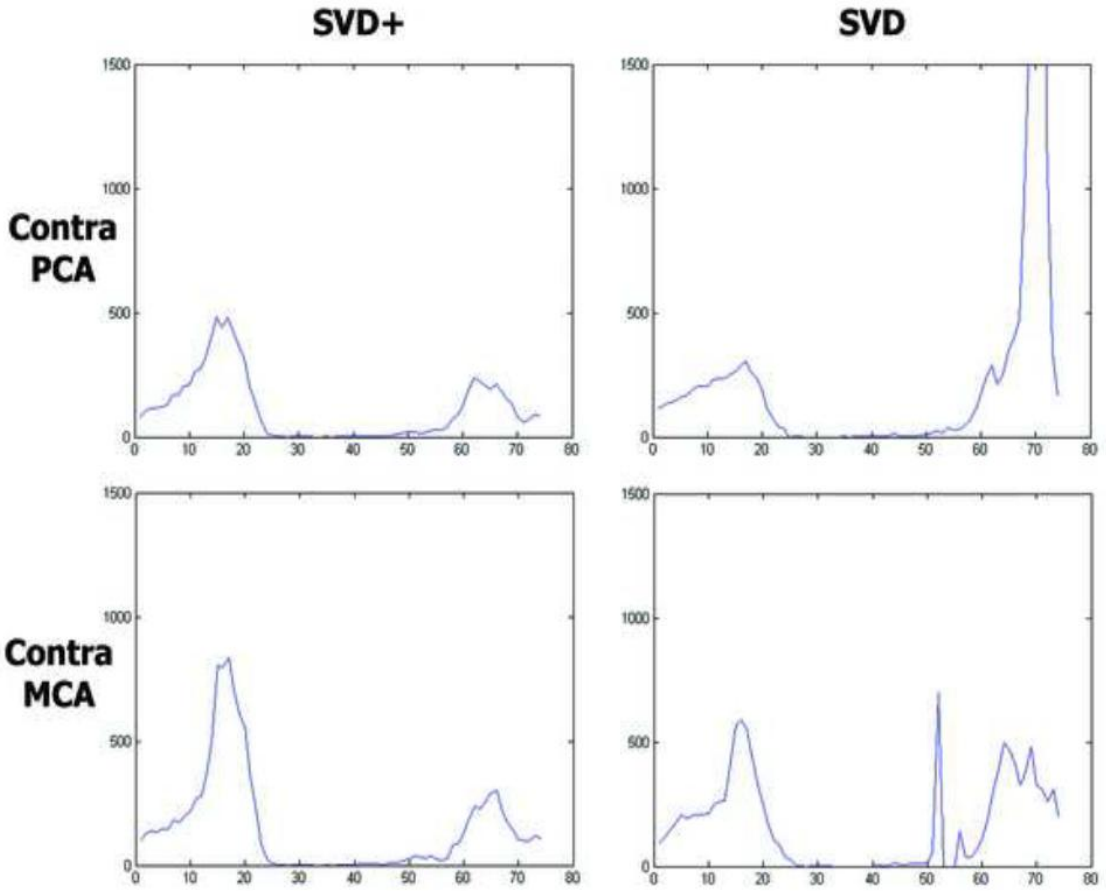

Selection	Contralateral Variation 1 (Contra PCA)	Contralateral Variation 2 (Contra MCA)
Arterial (AIF)	PCA	MCA
Venous (VIF)	SSS	SSS

Figure 10. 2D "linear pixel" graphs based on the linear selection in Figure 5. By varying the manual AIF selection in either the contralateral PCA or MCA (VIF held constant in the posterior SSS) this allows for quantitative comparison of CBF x CBV product values derived from the use of either the SVD+ or SVD deconvolution algorithms. Each pixel value represents 0.5 mm. The y-axis is the product of CBF x CBV pixel values at the same location. The x-axis is 80 linear pixels collected in the linear selection moving from lateral superior to the medial inferior aspects for the frontal lobe infarct.

3.4 Varying Location of VIF Selection (AIF Held Constant)

Varying the location of the VIF resulted in different results for all protocol configurations of both SVD and SVD+. The AIF was held constant in the MCA with a manual selection. The VIF was compared between the two locations of the SSS and CDVS. Results indicated less variation in the CBF x CBV product between the SVD+ 2D "slice pixel" maps for CDVS and posterior SSS. More variation in overall results was evident on the SVD produced 3D "slice voxel" maps and quantitative 2D "linear pixel" graphs when the VIF selection was changed.

Increased homogeneity of the infarct location was observed for the 2D "slice pixel" maps for CDVS when using SVD (Fig. 11). In regards to the 3D "slice voxel" map, the posterior SSS resulted in higher and more defined peaks than the CDVS. It was also shown that the collateral circulation of the infarcts was increased using both the CDVS and posterior SSS for SVD and less pronounced for SVD+. Both SVD+ and SVD 3D maps of the posterior SSS produced higher and more defined peaks than the CDVS selection creating a smoother overall image for interpretation purposes (Fig. 12). As with the results obtained by varying the AIF selection, the 2D "linear pixel" graphs (Fig. 13) indicated higher CBF x CBV product values. Again, using SVD, there was more variation in the CBF x CBV values and more poorly defined peaks.

3.5 CBF "Linear Pixel" Subtraction Graphs (SVD+ or SVD)

Larger differences were seen from the SVD versus SVD+ deconvolution protocol in regards to the AIF/VIF CTP values as explained previously. Subtraction of the manual AIF/VIF CTP values from the automatic AIF/VIF CTP values showed this larger variation with SVD than with SVD+ (Table 4). Additionally, the 2D "linear pixel"

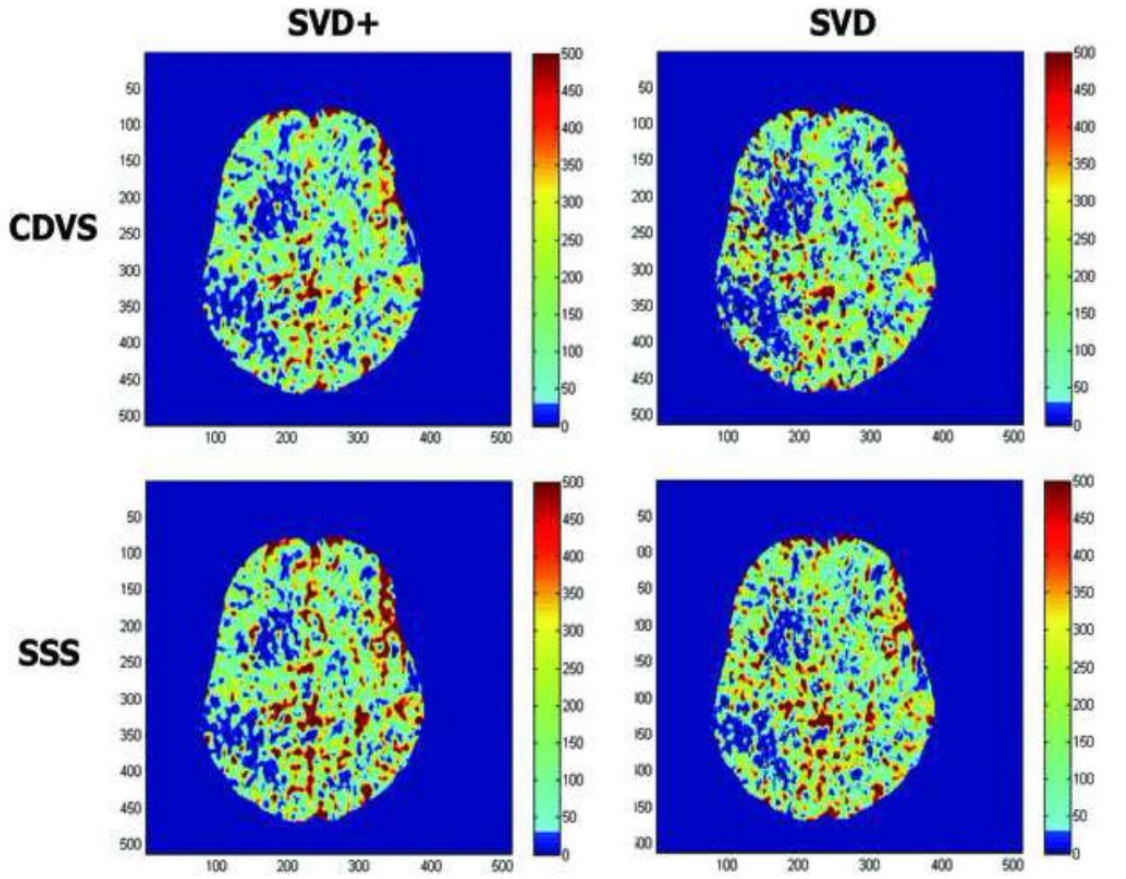

Selection	VIF Variation 1 (CDVS)	VIF Variation 2 (SSS)
Arterial (AIF)	MCA	MCA
Venous (VIF)	CDVS	SSS

Figure 11. . 2D "slice voxel" colorimetric maps were created to compare variation in CBF x CBV value outputs based on varying the VIF location either in CDVS or the posterior SSS location (AIF held constant in MCA) and SVD+/SVD variations.

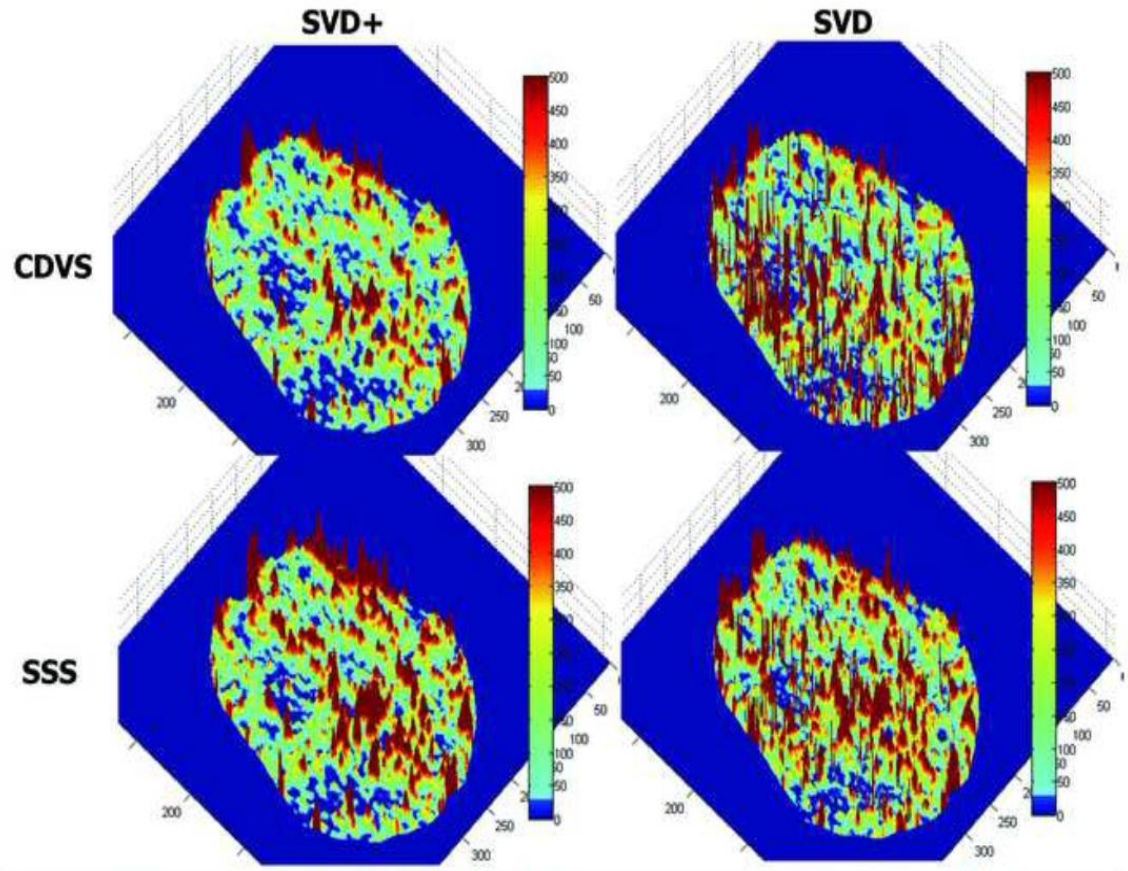

Selection	VIF Variation 1 (CDVS)	VIF Variation 2 (SSS)
Arterial (AIF)	MCA	MCA
Venous (VIF)	CDVS	SSS

Figure 12. 3D "slice voxel" colorimetric maps were created to compare variation CBF x CBV value outputs based on varying the VIF location either in CDVS or the posterior SSS location (AIF held constant in MCA) and SVD+/SVD variations.

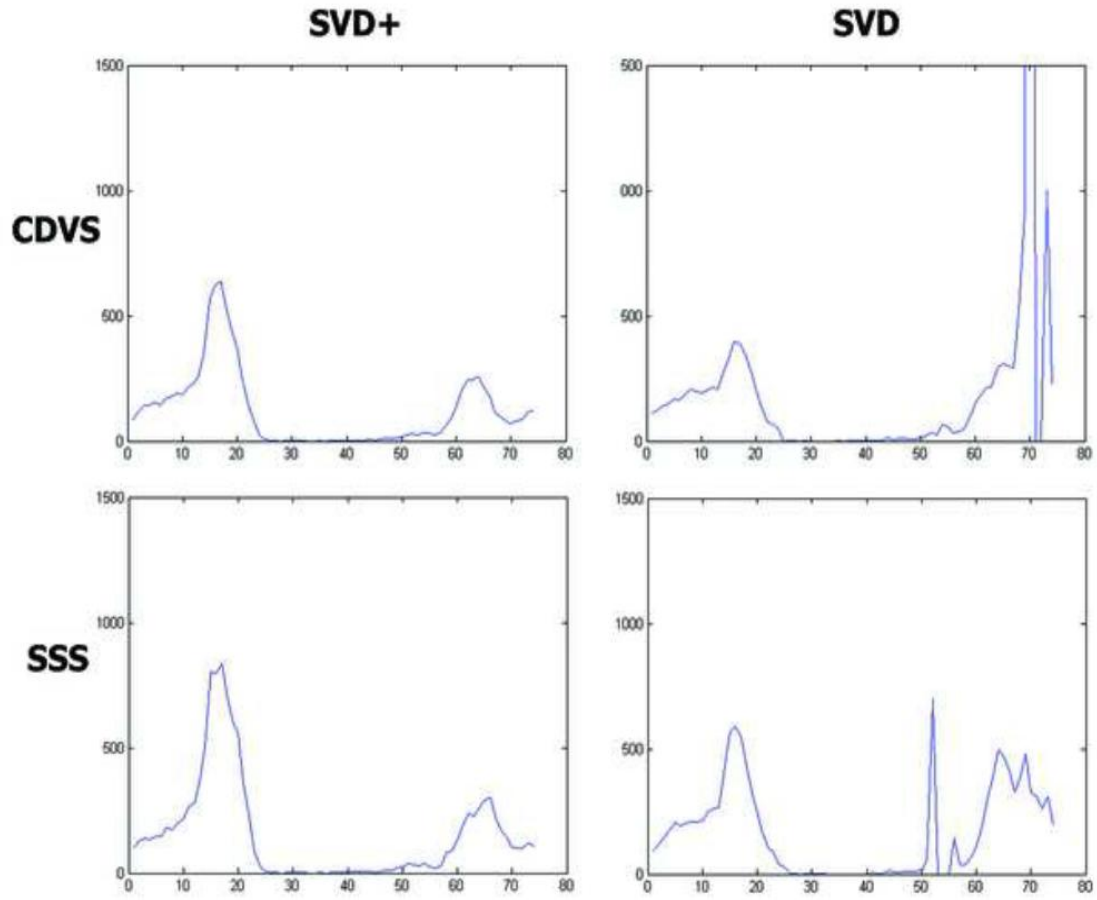

Selection	VIF Variation 1 (CDVS)	VIF Variation 2 (SSS)
Arterial (AIF)	MCA	MCA
Venous (VIF)	CDVS	SSS

Figure 13. 2D "linear pixel" graphs created to compare variation of CBF x CBV value outputs based on varying the VIF location either in the CDVS or the posterior SSS location (AIF held constant in MCA) and SVD+/SVD variations. Each pixel value represents 0.5 mm. The y-axis is the product of CBF x CBV pixel values at the same location. The x-axis is 80 linear pixels collected in the linear selection moving from lateral superior to the medial inferior aspects for the frontal lobe infarct.

subtraction graphs indicated larger variations of positive and negative CBF values for SVD versus SVD+ (Fig. 14a and 14b). In regards to the parameters involved for each

case analysis, CBF had by far the greatest variations of CTP values when compared to the other parameters of CBV, TTP, MTT, and delay values for both SVD and SVD+.

Variation between the manual AIF/VIF selection versus the automatic template AIF/VIF selection was compared to measure the differences between SVD and SVD+. The manually placed AIF/VIF was placed in the exact same position as the automatic template placed AIF/VIF location for variation analysis using the standard deviations of the CTP values generated. Using SVD+, the standard deviation in AIF/VIF selection differences for CBF ranged from 8.1 to 30.20. Using SVD, the standard deviations were higher and ranged from 55.97 to 605.91. The template-placed automatic selection subtracted from software-placed automatic selection demonstrated that both deconvolution methods are stable and that if AIF/VIF selections are identical, the resulting CTP values will be equal. This subtraction also served as our control to ensure MATLAB computations were correct.

For the other CTP parameters, CBV had SVD+ standard deviations that were lower than SVD and ranged from 0.11 (CDVS-Automatic) to 0.29 (operator placed automatic-automatic). SVD deviations ranged from 0.21 (contralateral PCA-automatic) to 0.67 (operator placed automatic-automatic). As expected, MTT demonstrated larger deviations using SVD as a result of delay variations. The delay variations affect SVD but not SVD+. TTP subtraction values were essentially unchanged for each AIF/VIF selection comparison using SVD+. This was expected as TTP values are independent of AIF/VIF selection when SVD+ is selected as the protocol in the workstation software. TTP was observed to be dependent on AIF/VIF selection when SVD is selected in the workstation software and this was not expected and suspected to be a result of an error in

Table 4. Statistical analysis of subtractions comparing manually selected AIF/VIF functions to automatic selection of AIF/VIF by software using SVD+ and SVD and various CTP parameters.

Contra - Auto (SVD+)	**CBV**	**CBF**	**TTP**	**MTT**
Mean	0.13	3.98	-0.00	0.03
Standard Deviation	0.16	13.34	0.01	0.86
Maximum	0.36	47.50	0.00	2.05
Minimum	-0.25	-20.50	-0.10	-2.18
Contra - Auto (SVD)	**CBV**	**CBF**	**TTP**	**MTT**
Mean	0.10	18.11	0.46	-0.73
Standard Deviation	0.35	81.42	6.00	2.06
Maximum	0.81	595.90	18.90	4.22
Minimum	-1.52	-195.80	-21.50	-8.61
Ipsi - Auto (SVD+)	**CBV**	**CBF**	**TTP**	**MTT**
Mean	0.12	12.24	-0.00	-0.28
Standard Deviation	0.23	26.53	0.01	1.04
Maximum	0.55	82.70	0.00	1.68
Minimum	-0.38	-16.10	-0.10	-2.51
Ipsi - Auto (SVD)	**CBV**	**CBF**	**TTP**	**MTT**
Mean	0.09	56.36	2.27	-1.34
Standard Deviation	0.40	174.62	7.42	2.38
Maximum	0.64	1401.60	22.80	4.74
Minimum	-2.04	-181.50	-14.80	-8.78
Contra (PCA) - Auto (SVD+)	**CBV**	**CBF**	**TTP**	**MTT**
Mean	-0.15	-1.52	-0.00	-0.02
Standard Deviation	0.16	11.00	0.01	0.85
Maximum	0.03	27.60	0.00	2.55
Minimum	-0.63	-28.50	-0.10	-2.40
Contra (PCA) - Auto (SVD)	**CBV**	**CBF**	**TTP**	**MTT**
Mean	-0.13	88.47	1.42	-0.33
Standard Deviation	0.21	399.38	6.81	2.17
Maximum	0.66	2361.00	22.80	5.08
Minimum	-0.63	-198.10	-18.90	-7.59

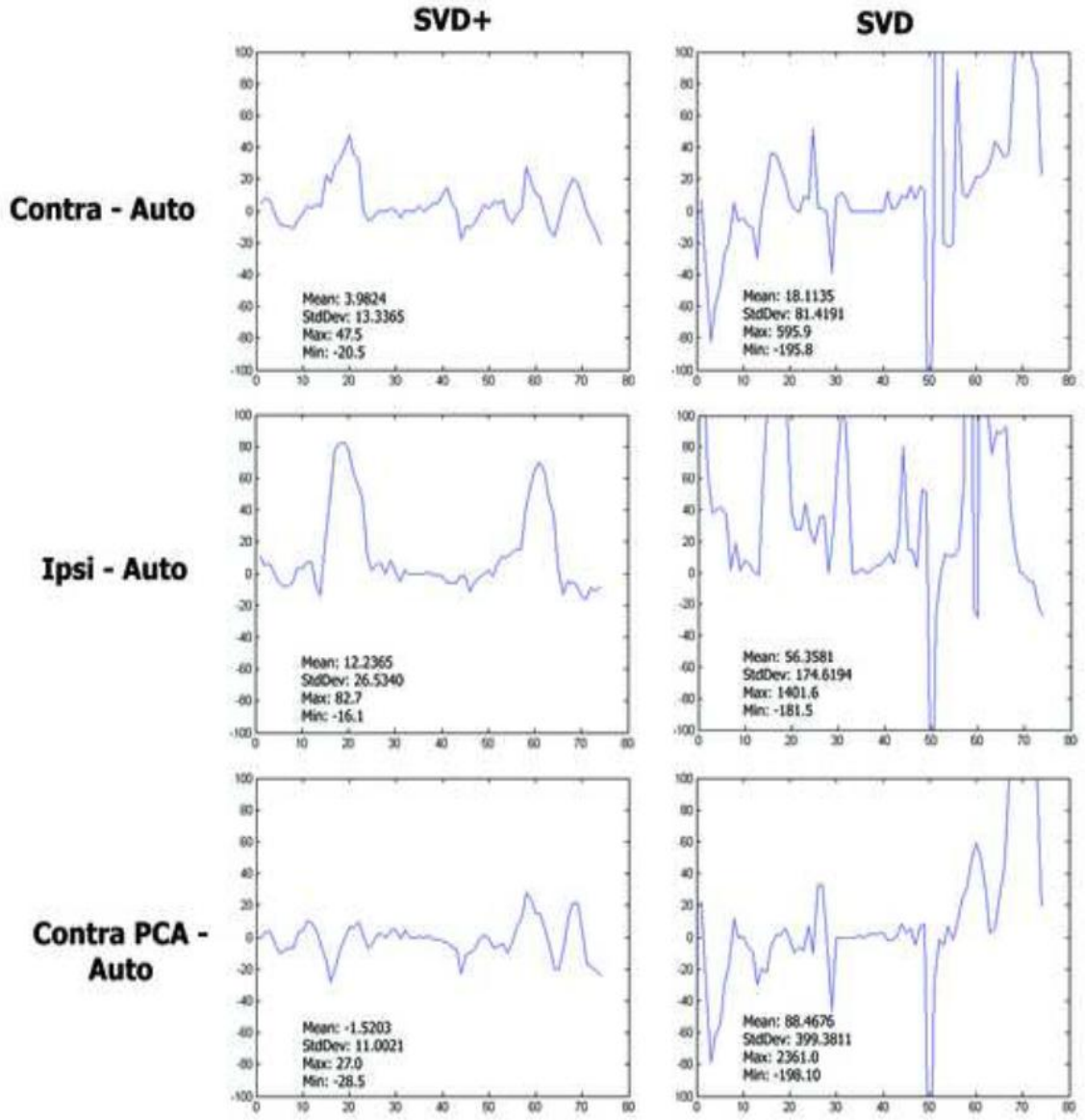

Selection	Automatic (Auto)	Ipsilateral (Ipsi)	Contralateral (Contra)	Contralateral (Contra PCA)
Arterial (AIF)	Contralateral PCA	PCA	MCA	PCA
Venous (VIF)	CDVS	SSS	SSS	SSS

Figure 14A. 2D "linear pixel" subtraction graphs that compare variations of CBF value outputs using either SVD+ or SVD by subtracting the AIF selection methods (contralateral MCA – automatic PCA, ipsilateral-automatic in PCA, contralateral in PCA-automatic in PCA; VIF was held constant in posterior SSS). Each pixel value represents 0.5 mm. The y-axis is the product of CBF x CBV pixel values at the same location. The x-axis is 80 linear pixels collected in the linear ROI moving from lateral superior to the medial inferior aspects for the frontal lobe infarct.

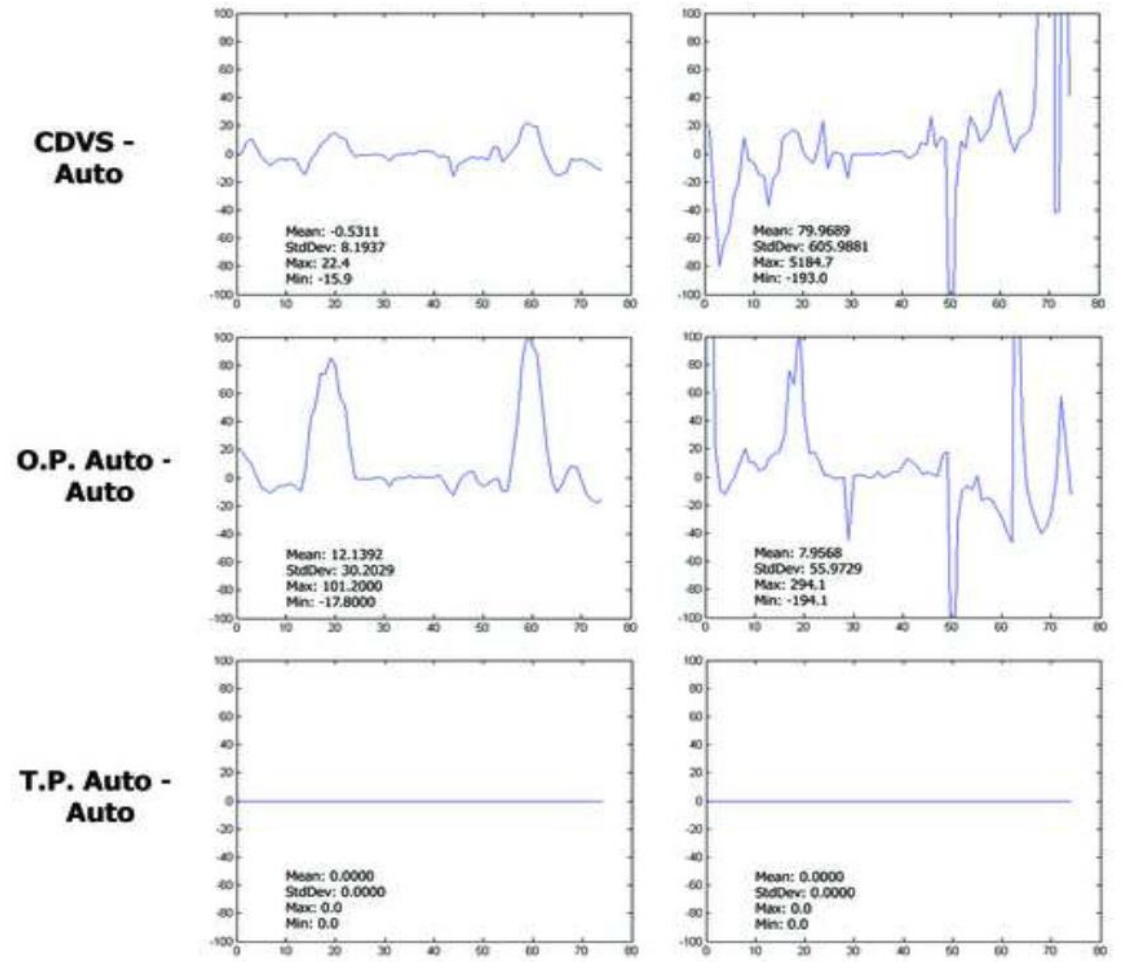

Selection	Automatic (Auto)	Contralateral (CDVS)	Operator Placed Automatic (O.P. Auto)	Template Placed Automatic (T.P. Auto)
Arterial (AIF)	Contralateral PCA	MCA	Contralateral PCA	Contralateral PCA
Venous (VIF)	CDVS	CDVS	CDVS	CDVS

Figure 14B. **.** 2D "linear pixel" subtraction graphs that compare variations of CBF value outputs using either SVD+ or SVD. To determine the influence of the posterior SSS VIF placement held constant in Figure 14a, the automatic CDVS selection (automatic AIF in the contralateral PCA) was subtracted from the manual CDVS VIF selection (AIF in the contralateral MCA). To demonstrate the effects of small changes in selection, automatic selections were manually placed by an operator (operator placed automatic) and then subtracted from automatic selection. Finally, a subtraction graph of two automatic placements on two different workstations was generated (template placed automatic). Each pixel value represents 0.5 mm. The y-axis is the product of CBF x CBV pixel values at the same location. The x-axis is 80 linear pixels collected in the linear ROI moving from lateral superior to the medial inferior aspects for the frontal lobe infarct.

the SVD algorithm for calculating TTP. Using SVD+, subtraction of the operator placed automatic AIF/VIF selection from the automatic selection, resulted in two increased peaks of standard deviation between core and penumbra on the 2D “linear pixel” subtraction graph (Fig 14b). The remainder of the graph showed that the core and normal tissue areas were relatively unchanged. This was also observed to a lesser extent when ipsilateral selection (AIF in the ipsilateral PCA, VIF in the posterior SSS) was subtracted from the automatic selection (Fig. 14a). This may be due to auto-regulation in the penumbra that affected both CBF and CBV values in a narrow region that neither deconvolution algorithm may be able to accurately compute. However, a large number of AIS cases will need to be examined to confirm this finding (Fig. 14b and Table 5).

3.6 Analysis of Multiple Cases

Analysis of AIS Cases 2-6 with 2D "slice voxel", "linear pixel" and 3D "slice voxel" figures is presented for qualitative comparison in Figure 15a and 15b. Quantitative 2D "linear pixel" graphs for Cases 2, 3, 4, and 6 demonstrated distinct CBF x CBV peaks on each edge of a central area of depressed values representing the presumed infarct core. Case 6 demonstrated inhomogeneity of the infarct blood flow and volume with three CBF x CBV peaks enclosing two depressions. The central peak of increased CBF x CBV values correspond with an increase in blood flow and volume in the center of the infarct in both of the 2D and 3D “slice voxel” colorimetric representations (Fig. 15a and 15b).

Case 5 did not have distinct peaks due to infarct heterogeneity and broad central hypoperfusion, but the area of infarct and ischemia can still be appreciated qualitatively. Case 6 was a 60-year-old female that did not have movement during the CT scan and demonstrates a generalized compensatory hemodynamic response throughout her brain.

Table 5. Statistical analysis of subtractions comparing manually selected AIF/VIF functions to automatic selections and the control subtraction (template placed automatic-automatic) of AIF/VIF using SVD+ and SVD and using various CTP parameters.

Contra (CDVS) - Auto (SVD+)	**CBV**	**CBF**	**TTP**	**MTT**
Mean	-0.07	-0.53	-0.00	0.00
Standard Deviation	0.11	8.19	0.01	0.67
Maximum	0.08	22.40	0.00	1.44
Minimum	-0.40	-15.90	-0.10	-1.98
Contra (CDVS) - Auto (SVD)	**CBV**	**CBF**	**TTP**	**MTT**
Mean	-0.10	79.97	1.25	-0.29
Standard Deviation	0.32	605.98	6.99	2.31
Maximum	0.72	5184.70	22.80	4.57
Minimum	-1.71	-193.00	-16.90	-9.21
O.P. Auto - Auto (SVD+)	**CBV**	**CBF**	**TTP**	**MTT**
Mean	-0.30	12.14	0.00	-0.57
Standard Deviation	0.29	30.20	0.00	1.03
Maximum	0.01	101.20	0.00	1.19
Minimum	-1.01	-17.80	0.00	-3.33
O.P. Auto - Auto (SVD)	**CBV**	**CBF**	**TTP**	**MTT**
Mean	-0.46	7.95	1.24	-0.72
Standard Deviation	0.67	55.97	8.65	2.87
Maximum	0.52	294.10	22.80	5.32
Minimum	-3.89	-194.10	-15.90	-7.06
T.P. Auto - Auto (SVD+)	**CBV**	**CBF**	**TTP**	**MTT**
Mean	0.00	0.00	0.00	0.00
Standard Deviation	0.00	0.00	0.00	0.00
Maximum	0.00	0.00	0.00	0.00
Minimum	0.00	0.00	0.00	0.00
T.P. Auto - Auto (SVD)	**CBV**	**CBF**	**TTP**	**MTT**
Mean	0.00	0.00	0.00	0.00
Standard Deviation	0.00	0.00	0.00	0.00
Maximum	0.00	0.00	0.00	0.00
Minimum	0.00	0.00	0.00	0.00

Case 7 had significant motion artifact even after removing one volume (volume 3) of the 19-volume acquisition data set and demonstrates the significant impact that motion in the remaining volumes can have on the resulting CTP values. Distinct CBF x CBV product peaks are not seen in Case 7, however, as with Case 5, the general infarct area

can still be qualitatively visualized. The quantitative CBF x CBV values in the z-axis in the 3D "slice voxel" images added additional clinical information (e.g., collateral circulation levels) for all cases that may not have been appreciated in the 2D "slice voxel" or axial CTP maps. Identifying the infarct area can be challenging for AIS cases, as seen in the 2D “slice voxel” map for Case 4 (Fig. 15a and 15b). However, results for cases 2-6 were qualitatively comparable to the deconvolution results of Case 1. Additionally, varying the AIF/VIF selection in Cases 2-7 yielded similar results as presented in the figures for Case 1.

3.7 Dose Reduction Analysis

The current DLP value for 19 volume acquisitions along with the estimated calculated effective dose for the corresponding number of volume acquisitions for each patient is shown in Table 6.

Decreasing the number of volume acquisitions from 19 to 18 volumes consequently decreased the effective dose by an average of 5.15%. The decrease in volume acquisitions from 19 to 17 resulted with the average corresponding effective dose decrease of 10.47%. The decrease from 19 to 16 volume acquisitions decreased the effective dose by an average of 15.75%. From 19 to 15 volume acquisition decrease, the average effective dose decreased by 21.09%. The average effective dose decrease by reducing the volume acquisitions from 19 to 14 was an average of 26.28%.

Qualitative analysis with the removal of one volume acquisition generated the same results in comparison to zero removal of volume acquisitions. The same is true with any number of volume acquisitions removed up to the descending base of the VIF bell curve of the time-intensity graph. The analysis of the qualitative 2D “slice pixel” CTP

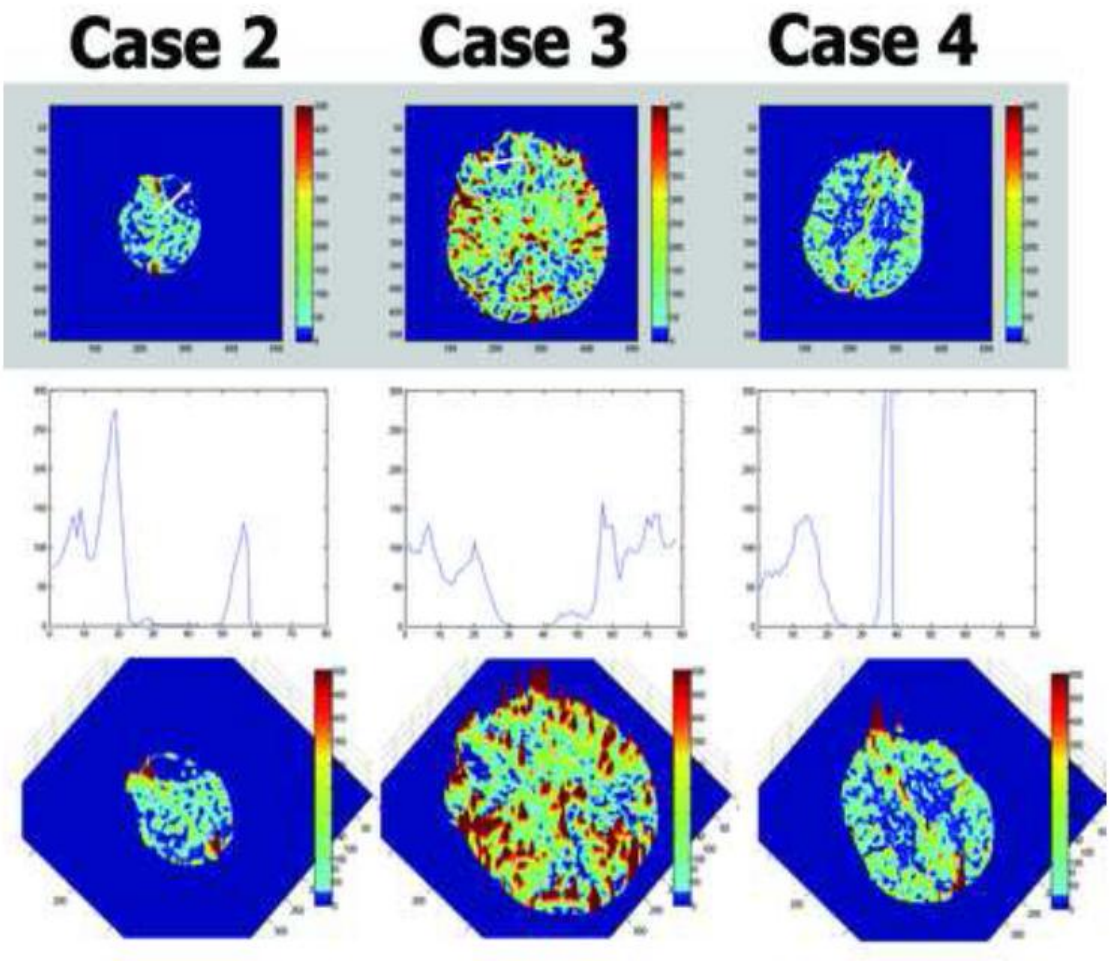

Figure 15a. Qualitative comparison of AIS Cases 2-4 with 2D "slice voxel", "linear pixel" and 3D "slice voxel" figures using SVD+.

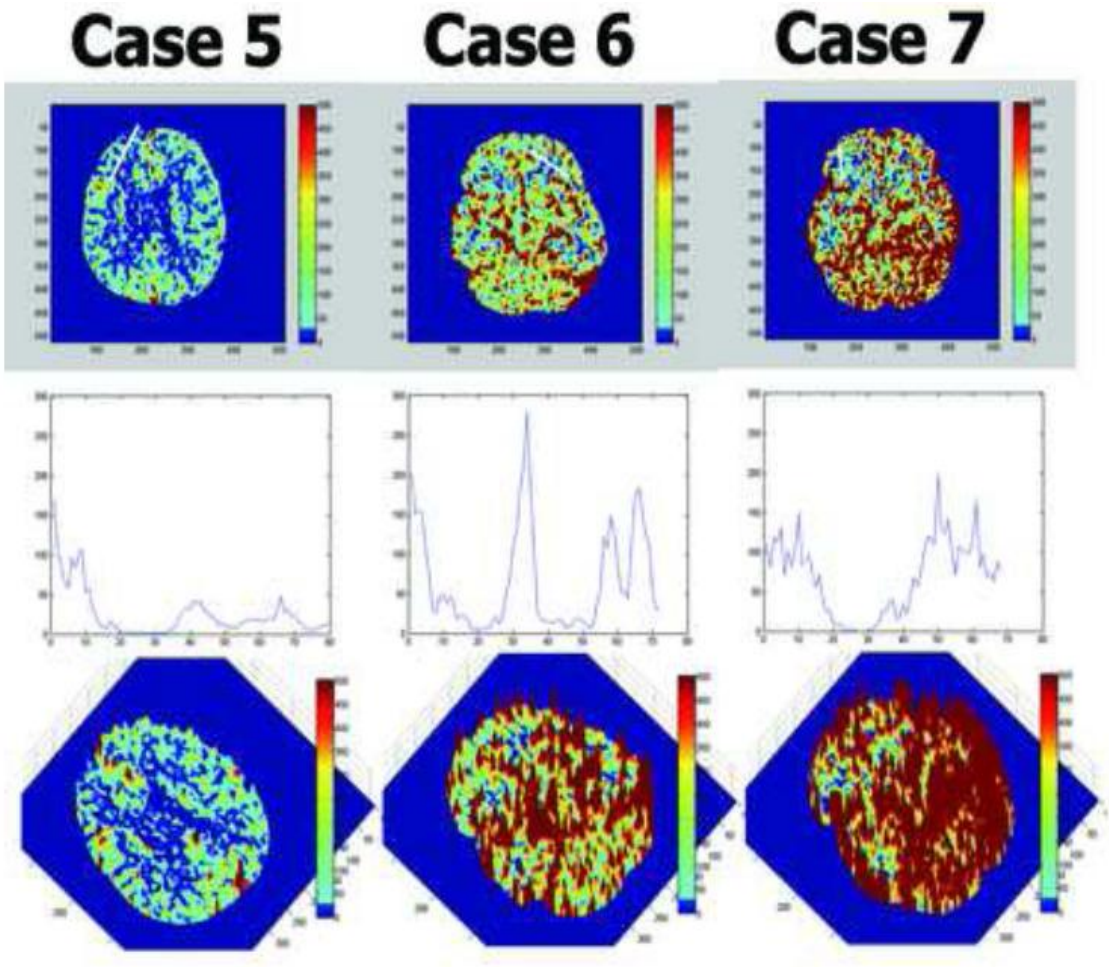

Figure 15b. Qualitative comparison of AIS Cases 5-7 with 2D "slice voxel", "linear pixel" and 3D "slice voxel" figures using SVD+.

Table 6. Effective dose in units of mSv for each case in regards to the corresponding number of volume acquisitions.

Case #	Dose Length Product (DLP)	19 Vol-Eff. Dose (mSv)	18 Vol-Eff. Dose (mSv)	17 Vol-Eff. Dose (mSv)	16 Vol-Eff. Dose (mSv)	15 Vol-Eff. Dose (mSv)	14 Vol-Eff. Dose (mSv)
000039	1957.6	4.50	4.27	4.03	3.79	3.55	3.32
000032	1957.6	4.50	4.27	4.03	3.79	3.55	3.32
000004	3174.8	7.30	6.92	6.53	6.15	5.76	5.38
000030	4392.0	10.10	9.57	9.04	8.51	7.97	7.44
000038	3174.8	7.30	6.92	6.53	6.15	5.76	5.38
000055	1884.0	4.33	4.11	3.88	3.65	3.42	3.19
000036	1957.6	4.50	4.27	4.03	3.79	3.55	3.32

maps indicated the same visual information for diagnostic capabilities.

Overall, according to the CTP values of the ROIs for each consistently placed template, the values do not change drastically with the removal of a volume acquisition prior to the descending base of the VIF bell curve. Once the volume acquisition number is reached that includes the base of the descending portion of the VIF bell curve, the CTP values tend to change drastically, resulting in an obvious change in the visual 2D “linear pixel” perfusion maps.

Line graphs of the CBF, CBV, and MTT ROI values for each different number of volume acquisitions indicate on average a fairly consistent CTP ROI value for the first two or three volume removals prior to a more drastic change in ROI values around the removal of three or four volume acquisitions (Fig. 16, 17, and 18).

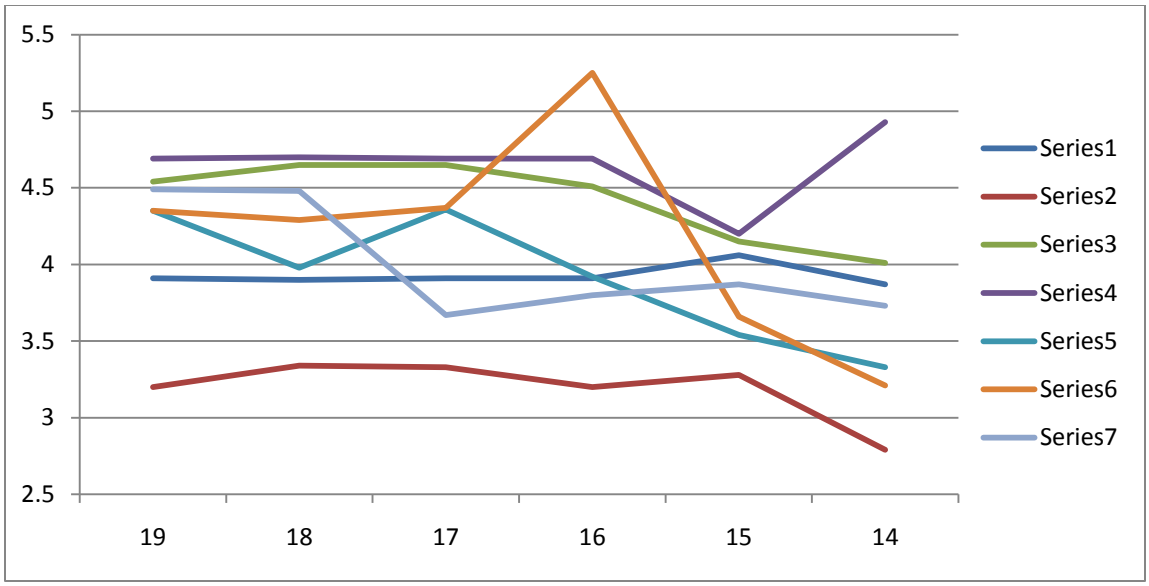

Figure 16. Line graph of the MTT ROI values versus the number of volume acquisitions for all seven cases.

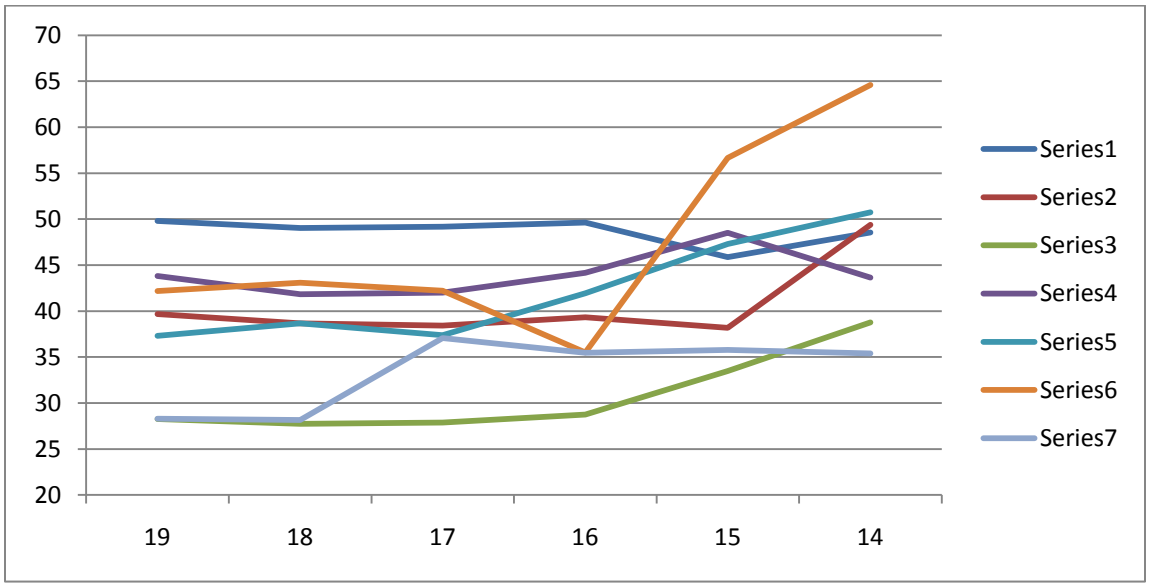

Figure 17. Line graph of the CBF ROI values versus the number of volume acquisitions for all seven cases.

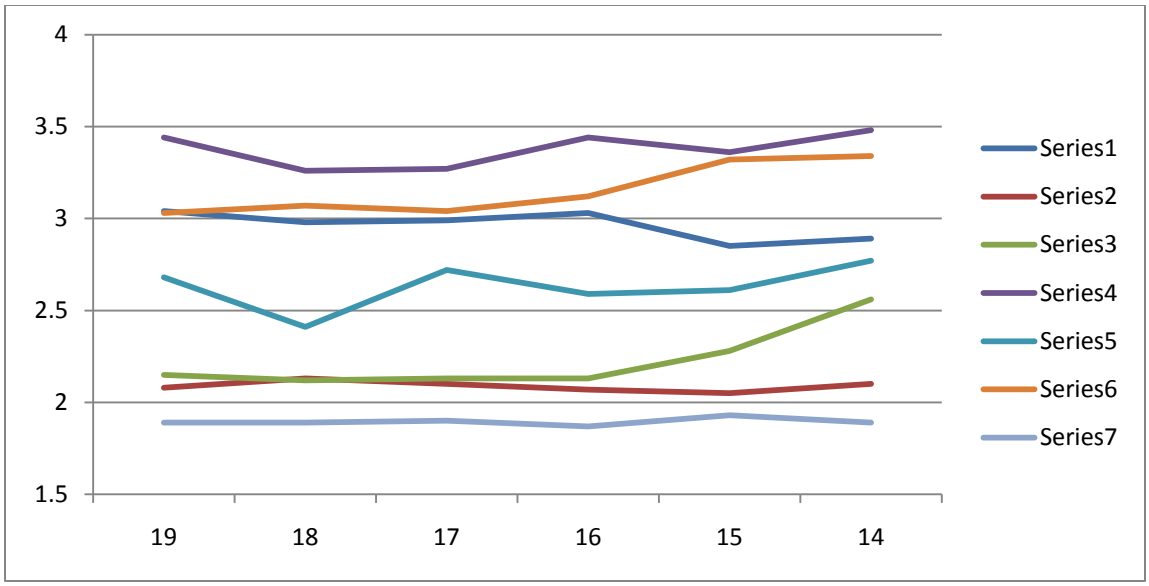

Figure 18. Line graph of the CBV ROI values versus the number of volume acquisitions for all seven cases.

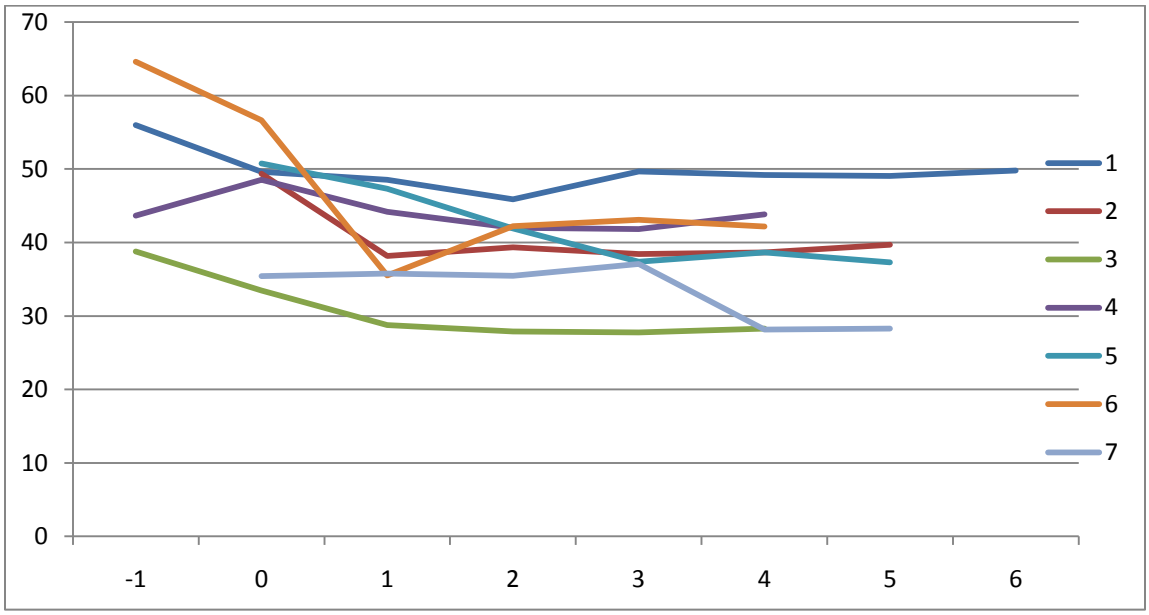

Figure 19. Line graph of the CBF-Shift ROI values versus the number of volume acquisitions. The graph shows the shift of each case curve to align the corresponding volume acquisitions with the base of the descending VIF bell curve.

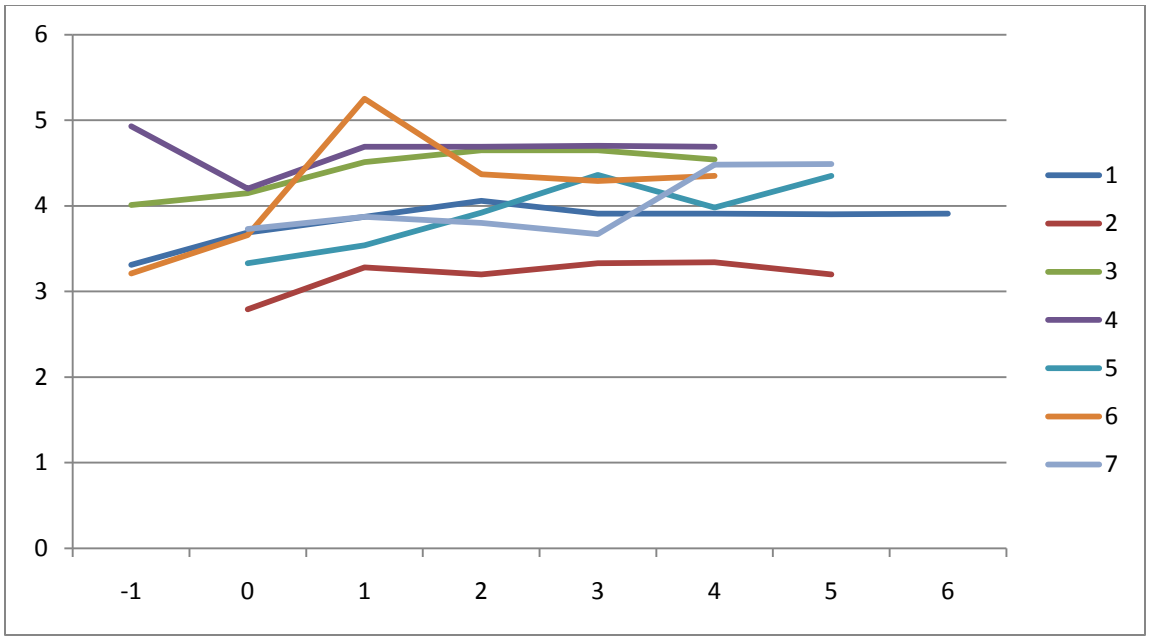

Figure 20. Line graph of the MTT-Shift ROI values versus the number of volume acquisitions. The graph shows the shift of each case curve to align the corresponding volume acquisitions with the base of the descending VIF bell curve.

CHAPTER 4

DISCUSSION

The clinical utility of CTP scanning for the diagnosis and analysis of an individual's current state of cerebral hemodynamics is a very important and necessary implementation for the assessment of AIS and other central nervous system conditions. The overall goals of this study were to assess the premier protocol using both qualitative and quantitative analysis for the comparison of SVD+ versus SVD and AIF and VIF variations.

Through the comparative analysis of the SVD+ versus the SVD deconvolution algorithms and the variation of the AIF and VIF locations, an accepted standard was implemented and will hopefully be used throughout the field of radiology and neurologic disorders. From experimentation and study, the SVD+ deconvolution protocol produced more accurate and consistent perfusion mapping with more defined graphical results and data. Full analysis of each AIS case supported this overall study and results.

4.1 SVD+ versus SVD Impact on CTP Values

In this study, SVD+ produced overall more consistent CTP values with less variation than SVD. Qualitatively, there was less variation with SVD+ than SVD during the variation of AIF and VIF selections. Qualitative analysis of the 3D perfusion maps indicated more defined peaks and penumbral boundaries with consistency and contiguity using SVD+ versus SVD. Additionally, the 2D "linear pixel" graphs created using SVD+ produced a more consistent and smoother outline in regards to variation in CBF x CBV values of the possible infarcted core and penumbral boundaries than SVD.

It is important to be aware that even though SVD+ tended to produce more consistent qualitative and quantitative CTP parameters, this does not create concrete

evidence of the most biologically accurate method. A large case study analysis would need to be conducted in order to verify these results, inclusive of follow up CT/MRI images. These images would allow for pathological along with the qualitative and quantitative analysis of the infarcted core and the penumbral boundaries. This would lead to the identification of the recovering penumbra and the penumbra leading to infarcted core. The infarct core range of values for CBV and CBF perfusion values in AIS for 320-detector row CT scanners has not been published at this time. The CBF x CBV value range would be determined with a large case analysis with the protocol variation of SVD+ and SVD and AIF/VIF selection.

By evaluating a set of quantitative 2D "linear pixel" graphs, presumed penumbral and infarct core boundaries were visible through the corresponding changes of the 2D graph. There were generally two sharp peaks with a very small full width at half maximum at each end depicting the normal area separated by a depressed central area that represented the core and the penumbra of the lesion. Compared to SVD+, there was large deviation of SVD-derived CTP parameters in the brain tissue region outside of the ischemic penumbra with high standard deviations.

4.2 AIF and VIF Selection Variation

As seen in the 2D “linear pixel” graphs, automatic and manual selection methods for AIF and VIF created only minor differences in 3D perfusion maps using SVD+ while the AIF and VIF selections using SVD generated much larger differences in the 3D perfusion maps. The SVD algorithm demonstrated large differences of CTP values depending on the AIF selection location. Manual contralateral AIF selection of the MCA led to higher CBF x CBV values compared to when the AIF was selected in the PCA.

Additionally, there were an increased number of CBF x CBV peaks in the 3D "slice voxel" maps in the collateral circulation areas around the medial and lateral aspects of the frontal and parietotemporal lobe infarct areas for MCA using SVD and diffusely increased CBF x CBF map values for the MCA selection using SVD+ (Fig. 9). It has been previously reported that choice of a large proximal intracranial artery compared to a smaller distal diameter artery did not affect CTP values in a study of three patients[29], but a possible contributing factor to the higher CBF CTP values for the MCA could be the larger luminal diameter of the M1 segment of the MCA of 3-5 mm while the P1 segment of the PCA is 1-3 mm[30]. Manual ipsilateral AIF selection did not differ qualitatively from manual contralateral AIF selection; however frequently in AIS cases the ipsilateral selection is not always possible in the MCA due to occlusion of this artery.

Overall, SVD+ qualitatively decreased the noise and variability in the CTP parameters when compared to SVD. Additional research on automatic AIF and VIF compared to manual selection variations is required in a larger numbers of patients without abnormalities and for condition-specific hemodynamics including AIS. Further research is also required on a larger number of AIS cases to verify and validate these initial results.

No guidelines are available to clinicians for recommending the correct side of the AIF selection in relation to the affected hemisphere in AIS. One study stated that the selection of a contralateral vessel might lead to an overestimate of hemodynamic injury while ipsilateral selection could lead to quantitative CTP overestimates.[9] In a review of the technical implementations of CTP and acute stroke studies it was suggested that there was no significant influence on CBV, CBF and MTT based on AIF laterality when using

delay insensitive deconvolution algorithms.[26] Another study found that infarct core and penumbra CBV, CBF and MTT values were highly correlated between contralateral and ipsilateral AIF selections when using a delay insensitive deconvolution algorithm.[31] Our findings suggest that this may be true when viewing 2D qualitative colorimetric maps; however the 2D subtraction graphs (Fig 14a) revealed differences when comparing ipsilateral PCA selections with the contralateral PCA selection in the region of the ischemic penumbra. Differences in CBF values were also observed when comparing selections with very small spatial differences (operator placed automatic selection – automatic selection) (Fig 14b). This may be caused by increased CBF values of the penumbra surrounding the infarct core. CBV and MTT values were not different when comparing laterality. Additional studies for determining the affect of AIF laterality on the resulting CTP values for baseline and disease states with significant hemodynamic changes are required to provide needed guidance on this topic.

In this study, the location of the VIF selection was varied between the CDVS and the posterior SSS with the AIF held constant in the MCA for both 2D and 3D "slice voxel" maps. The CBF x CBV product values were analyzed using both the SVD+ and SVD deconvolution algorithms to evaluate the impact of the VIF location. It has been shown that choosing the VIF with the highest peak enhancement value increases the signal-to-noise ratio and decreases variability in CTP values.[32] It is also known that sensitivity of the CTP outputs based on the settings can vary widely with workstation software.[29] Scanning artifacts were observed near the pituitary fossa due to bony protrusions and may possibly impact CTP variations if near the VIF in the CDVS. All of

these possible sources of variation demonstrate that it is important to understand the influence of the VIF on each patient's CTP images.

For the cases that were analyzed, the accepted approach for our analysis consisted of the AIF and VIF selection process of selecting the AIF in the contralateral M1 segment of the MCA to the infarcted hemisphere and the VIF selected in the posterior portion of the SSS. Keeping these locations consistent throughout can reduce the variations introduced by software, the act of selecting different vascular anatomy, reducing AIF laterality, and artifact influence in VIF. Future studies must include individual variations inclusive of age, sex, cardiac output, and hematocrit, along with quantitative analysis of variations in deconvolution results to determine the impact of these factors on clinical image interpretations for different CNS diseases, especially AIS.[33]

On a much broader national and international scale, the adoption of standard guidelines for the clinical use of CTP in varied CT systems is necessary to facilitate comparison between studies on CTP parameter values.[10,24] To facilitate comparisons between CTP protocols used and for adequate reporting of radiation doses, a format for CTP hardware, software, protocol and scan configuration parameters is suggested previously in this writing. Including this basic information in CTP publications would facilitate improved comparisons of CTP data between institutions and across vendors. It has been shown that MTT and CBF values are significantly different among different CT brain perfusion software vendors.[34,35] Additionally, the absolute calibration of CTP parameters is a necessity for inter-software consistency.[36,37]

4.3 Dose Reduction

The plotted CBF, CBV, and MTT values of the template of ROIs indicate an overall trend of consistency with the removal of one or more volume acquisitions up to the base of the VIF bell curve. Further analysis with a large case number evaluation would need to be conducted to follow up on these preliminary results. Further analysis would need to consist of possibly a greater number of ROIs in the template along with consistency of the AIF and VIF selection locations for AIS cases.

Overall, according to the results of the decrease of volume acquisitions from the end of the scanning process, it would be safe to recommend an 18-volume acquisition protocol in place of the current 19-volume acquisition protocol. This would result in the same qualitative and very similar quantitative results necessary for accurate diagnosis and prognosis of the AIS cases. Further volume acquisition removal may be warranted with further and more intensive, comprehensive case study.

CHAPTER 5

CONCLUSIONS

In this study of protocol variation analysis, SVD+ proved to have more consistent CTP values with less variation than the SVD deconvolution algorithm. With the use of the SVD+ deconvolution algorithm, the most consistent results were produced with the AIF manually placed in the contralateral M1 segment of the MCA and the VIF placed in the posterior portion of the SSS. This protocol is the suggested approach for clinical methodology to minimize input variation and produce the most accurate results. Developing a consistent approach will lead to comparative analyses with a larger case study and allow for clinicians to adopt an accepted scanning and reading protocol. Experience in defining and specifying the boundaries of the ischemic penumbra and core infarcted areas will allow the reader to provide consistent diagnoses and prognoses.

The use of whole-brain CTP and the advances of this technology will hopefully lead to an extended time window for the use of drugs like tPA for the revascularization of the stroke-affected tissue.[38] This time window could possibly be extended to be more patient specific and decreasing the possibility of complication due to administration of the drugs. These advances may also lead to the treatment of other CNS diseases including crossed cerebellar diaschisis and allow for a more accurate prognosis.

5.1 Study Limitations

The analysis methods utilized for this study require software and processes (e.g., switching between SVD+ and SVD) not included in the workstation software and necessitates access to the workstation to complete the computationally intensive process of pixel-by-pixel slice level or 3D analysis of CT perfusion parameter data. Determining

the range of expected infarct core and penumbra values for the 320-detector row CT was not included in this study. Ultimately, a large collection of these CTP values derived from comparison methods used in this study combined with the follow up CT/MRI or pathology studies is required to confirm the findings presented.

BIBLIOGRAPHY

1. Bushberg J, Seibert J.A., Leidholdt E, Boone J. The Essential Physics of Medical Imaging. Lippincott Williams & Wilkins. 2002;327-372.

2. Wintermark M, Flanders AE, Velthuis B, et al. Perfusion-CT assessment of infarct core and penumbra: receiver operating characteristic curve analysis in 130 patients suspected of acute hemispheric stroke. Stroke. Apr 2006;37(4):979-985.

3. Schaefer PW, Barak ER, Kamalian S, et al. Quantitative assessment of core/penumbra mismatch in acute stroke: CT and MR perfusion imaging are strongly correlated when sufficient brain volume is imaged. Stroke. Nov 2008;39(11):2986-2992.

4. Saver JL. Time is brain--quantified. Stroke. Jan 2006;37(1):263-266.

5. Rothwell PM. Prediction and prevention of stroke in patients with symptomatic carotid stenosis: the high-risk period and the high-risk patient. Eur J Vasc Endovasc Surg. Mar 2008;35(3):255-263.

6. Wardlaw JM, Murray V, Berge E, et al. Thrombolysis for acute ischemic stroke. Cochrane Database Syst Rev. 2009(4):CD000213.

7. Schellinger PD, Fiebach JB, Mohr A, et al. Thrombolytic therapy for ischemic stroke—a review. Part I--Intravenous thrombolysis. Crit Care Med. Sep 2001;29(9):1812-1818.

8. Wintermark M. Brain perfusion-CT in acute stroke patients. European Radiology. 2005;15 Suppl 4:D28-31-D28-31.

9. Cianfoni A, Colosimo C, Basile M, et al. Brain perfusion CT: principles, technique and clinical applications. La Radiologia Medica. 2007;112(8):1225-1243.

10. Konstas AA, Goldmakher GV, Lee TY, et al. Theoretic basis and technical implementations of CT perfusion in acute ischemic stroke, part 1: Theoretic basis. AJNR Am J Neuroradiol. Apr 2009;30(4):662-668.

11. Ostergaard L. Principles of cerebral perfusion imaging by bolus tracking. J Magn Reson Imaging. Dec 2005;22(6):710-717.

12. Wintermark M, Thiran JP, Maeder P, et al. Simultaneous measurement of regional cerebral blood flow by perfusion CT and stable xenon CT: a validation study. AJNR Am J Neuroradiol. May 2001;22(5):905-914.

13. Calamante F, Gadian DG, Connelly A. Delay and dispersion effects in dynamic susceptibility contrast MRI: simulations using singular value decomposition. Magn

Reson Med. Sep 2000;44(3):466-473.

14. Murase K, Shinohara M, Yamazaki Y. Accuracy of deconvolution analysis based on singular value decomposition for quantification of cerebral blood flow using dynamic susceptibility contrast-enhanced magnetic resonance imaging. Phys Med Biol. Dec 2001;46(12):3147-3159.

15. Eastwood JD, Lev MH, Azhari T, et al. CT perfusion scanning with deconvolution analysis: pilot study in patients with acute middle cerebral artery stroke. Radiology. Jan 2002;222(1):227-236.

16. Smith MR, Lu H, Trochet S, et al. Removing the effect of SVD algorithmic artifacts present in quantitative MR perfusion studies. Magn Reson Med. Mar 2004;51(3):631-634.

17. Wu O, Ostergaard L, Weisskoff RM, et al. Tracer arrival timing-insensitive technique for estimating flow in MR perfusion-weighted imaging using singular value decomposition with a block-circulant deconvolution matrix. Magn Reson Med. Jul 2003;50(1):164-174.

18. Kudo K, Sasaki M, Ogasawara K, et al. Difference in tracer delay-induced effect among deconvolution algorithms in CT perfusion analysis: quantitative evaluation with digital phantoms. Radiology. Apr 2009;251(1):241-249.

19. Preim B, Oeltze S, Mlejnek M, et al. Survey of the visual exploration and analysis of perfusion data. IEEE Trans Vis Comput Graph. Mar-Apr 2009;15(2):205-220.

20. Wintermark M, Maeder P, Thiran JP, et al. Quantitative assessment of regional cerebral blood flows by perfusion CT studies at low injection rates: a critical review of the underlying theoretical models. Eur Radiol. 2001;11(7):1220-1230.

21. Kudo K, Terae S, Katoh C, et al. Quantitative cerebral blood flow measurement with dynamic perfusion CT using the vascular-pixel elimination method: comparison with H2(15)O positron emission tomography. AJNR Am J Neuroradiol. Mar 2003;24(3):419-426.

22. Ibaraki M, Shimosegawa E, Toyoshima H, et al. Tracer delay correction of cerebral blood flow with dynamic susceptibility contrast-enhanced MRI. J Cereb Blood Flow Metab. Mar 2005;25(3):378-390.

23. Ostergaard L, Weisskoff RM, Chesler DA, et al. High resolution measurement of cerebral blood flow using intravascular tracer bolus passages. Part I: Mathematical approach and statistical analysis. Magn Reson Med. Nov 1996;36(5):715-725.

24. Sanelli PC, Nicola G, Tsiouris AJ, et al. Reproducibility of postprocessing of quantitative CT perfusion maps. Ajr. Jan 2007;188(1):213-218.

25. Lee TY, Murphy B, Chen X, et al. Image Processing. In: Miles KA, Eastwood JD, Konig M, eds. Multidetector Computed Tomography in Cerebrovascular Disease, CT Perfusion Imaging. London: Informa Healthcare Ltd.; 2007:64-67.

26. Konstas AA, Goldmakher GV, Lee TY, et al. Theoretic Basis and Technical Implementations of CT Perfusion in Acute Ischemic Stroke, Part 2: Technical Implementations. AJNR Am J Neuroradiol. Mar 19 2009.

27. Bongartz G, Golding SJ, Jurik AG, et al. European Guidelines for Multislice Computed Tomography: European Commission;2004.

28. Lee TY. Scientific basis and validation. In: Miles KA, Eastwood JD, Konig M, eds. Multidetector Computed Tomography in Cerebrovascular Disease, CT Perfusion Imaging. London: Informa Healthcare Ltd.; 2007:13-27.

29. Sanelli PC, Lev MH, Eastwood JD, et al. The effect of varying user-selected input parameters on quantitative values in CT perfusion maps. Acad Radiol. Oct 2004;11(10):1085-1092.

30. Grand W. Microsurgical anatomy of the proximal middle cerebral artery and the internal carotid artery bifurcation. Neurosurgery. 1980(7):215-218.

31. Bisdas S, Konstantinou GN, Gurung J, et al. Effect of the arterial input function on the measured perfusion values and infarct volumetric in acute cerebral ischemia evaluated by perfusion computed tomography. Invest Radiol. Mar 2007;42(3):147-156.

32. Kealey SM, Loving VA, Delong DM, et al. User-defined vascular input function curves: influence on mean perfusion parameter values and signal-to-noise ratio. Radiology. May 2004;231(2):587-593.

33. Turk AS, Johnson KM, Lum D, et al. Physiologic and anatomic assessment of a canine carotid artery stenosis model utilizing phase contrast with vastly undersampled isotropic projection imaging. AJNR Am J Neuroradiol. Jan 2007;28(1):111-115.

34. Koenig M, Klotz E, Luka B, et al. Perfusion CT of the brain: diagnostic approach for early detection of ischemic stroke. Radiology. Oct 1998;209(1):85-93.

35. Konig M. Brain perfusion CT in acute stroke: current status. Eur J Radiol. Mar 2003;45 Suppl 1:S11-22.

36. Gillard JH, Antoun NM, Burnet NG, et al. Reproducibility of quantitative CT perfusion imaging. Br J Radiol. Jun 2001;74(882):552-555.

37. Sa De Camargo EC, Koroshetz WJ. Neuroimaging of ischemia and infarction. NeuroRx. 2005;2(2):265-276.

38. Cohnen M, Wittsack HJ, Assadi S, et al. Radiation exposure of patients in comprehensive computed tomography of the head in acute stroke. American Journal of Neuroradiology. 2006;27(8):1741-1745.

VITA

Graduate College
University of Nevada, Las Vegas

Peter T. Heiberger

Degrees:

Bachelor of Science, Kinesiology, 2006
University of Wisconsin, Eau Claire

Thesis Title: Protocol Variation Analysis of Whole Brain CT Perfusion in Acute Ischemic Stroke

Thesis Examination Committee:

Chairperson, Dr. Steen Madsen, Ph.D.
Committee Member, Dr. Phillip Patton, Ph.D.
Committee Member, Dr. Ralf Sudowe, Ph.D.
Graduate Faculty Representative, Dr. Merrill Landers, Ph.D.